The seismo-hydro-mechanical behaviour during deep geothermal reservoir stimulations: open questions tackled in a decameter-scale in-situ stimulation experiment

Amann Florian[1)], Valentin Gischig[2)], Keith Evans[2)], Joseph Doetsch[2)], Reza Jalali[2)], Benoît Valley[3)] Hannes Krietsch[2)], Nathan Dutler[3)], Linus Villiger[2)], Bernard Brixel[2)], Maria Klepikova[2)], Anniina Kittilä[2)], Claudio Madonna[2)], Stefan Wiemer[2)], Martin O. Saar[2)], Simon Loew[2)], Thomas Driesner[2)], Hansruedi Maurer[2)], Domenico Giardini[2)],

[1)]RWTH Aachen, Chair of Engineering Geology and Hydrogeology, Lochnerstrasse 4-20, 52064 Aachen, Germany

[2)]ETH Zurich, Department of Earth Sciences, Sonneggstrasse 5, 8092 Zurich, Switzerland

[3)]University of Neuchatel, Centre for Hydrogeology and Geothermics (CHYN), Laboratory of Geothermics and Reservoir Geomechanics, 2000 Neuchâtel, Switzerland

Keywords: Deep geothermal energy, EGS, induced seismicity, in-situ experiments, hydro-mechanical coupled processes in EGS,

Abstract

In this contribution, we present a review of scientific research results that address seismo-hydro-mechanical coupled processes relevant for the development of a sustainable heat exchanger in low permeability crystalline rock and introduce the design of the In-situ Stimulation and Circulation (ISC) experiment at the Grimsel Test Site dedicated to study such processes under controlled conditions. The review shows that research on reservoir stimulation for deep geothermal energy exploitation has been largely based on laboratory observations, large-scale projects and numerical models. Observations of full-scale reservoir stimulations have yielded important results. However, the limited access to the reservoir and limitations in the control on the experimental conditions during deep reservoir stimulations is insufficient to resolve the details of the hydro-mechanical processes that would enhance process understanding in a way that aids future stimulation design. Small scale laboratory experiments provide fundamental insights into various processes relevant for enhanced geothermal energy, but suffer from 1) difficulties and uncertainties in upscaling the results to the field-scale and 2) relatively homogeneous material and stress conditions that lead to an over-simplistic fracture flow and/or hydraulic fracture propagation behaviour that is not representative for a heterogeneous reservoir. Thus, there is a need for intermediate-scale hydraulic stimulation experiments with high experimental control that bridge the various scales, and for which access to the target rock mass with a comprehensive monitoring system is possible. Only few intermediate-scale hydro-shearing and hydro-fracturing experiments have recently been performed in a densely instrumented rock mass. No such measurements have been performed on faults in crystalline basement rocks. The In-situ Stimulation and Circulation (ISC) experiment is designed to address open research questions in a naturally fractured and faulted crystalline rock mass at the Grimsel Test Site (Switzerland). Two hydraulic injection phases were executed to enhance the permeability of the rock mass: a hydro-shearing phase and then a hydraulic fracturing phase. During the injection phases the rock mass deformation across fractures and within intact rock, the pore pressure distribution and propagation and the micro-seismic response were monitored at a high spatial and temporal resolution.

1 Introduction

The necessity to produce carbon dioxide neutral electricity, ideally as base-load power (i.e., 24 hours a day, year-round) and the increased aversion to nuclear power generation have motivated global efforts to optimize methods for extracting deep geothermal energy for electricity production. However, currently, geothermal power production is limited to distinct geological conditions, where fluid flow rate in geothermal reservoirs carry sufficient heat (Saar, 2011) and/or pressure for economic power generation (Randolph and Saar, 2011a; Breede et al., 2013; Adams et al., 2015). It is widely agreed that the earth's crust holds substantially more geothermal resources than are presently being exploited (e.g., Tester et al., 2006). However, standard water- or brine-based geothermal power generation requires persistent high reservoir permeabilities of at least 10^{-16} m^2 (Manning and Ingebritsen, 1999) and temperatures of ideally over about 170°C (e.g., Evans, 2014; Saar, to be published in 2017), as otherwise it is not economic. Wells have to be drilled to at least 5 to 6 km depth into crystalline hard rock to reach formation temperatures of approximately 170-200°C in regions with standard geothermal gradients of about 30°C/km, although such temperatures are often reached at shallower depth if there is a low thermal conductivity sedimentary cover. Presently, rotary drilling to such depths is uneconomic on a routine basis. Moreover, at this depth, permeability is often much less than 10^{-16} m^2 (e.g., Manning and Ingebritsen, 1999; Saar and Manga, 2004), so that permeability has to be artificially enhanced to permit circulation of fluids to advectively extract the heat economically. Such systems are referred to as Enhanced or Engineered Geothermal Systems (EGS), originally termed Hot Dry Rock (HDR) systems (Brown et al., 2012). EGSs virtually always require hydraulic stimulation to enhance the permeability to such a degree that economic geothermal power generation becomes possible. However, the goal of controlling the permeability enhancement process has not yet been achieved in a sustained way, despite attempts since the 1970s (Evans, 2014). Additionally, induced seismicity, which almost invariably accompanies hydraulic stimulation because of the high fluid injection pressures, can be problematic inasmuch as it may reach felt or even damaging intensities (e.g., Giardini, 2009).

In this contribution, we focus on how a subsurface heat exchanger may be constructed between boreholes at depth within low-permeability rock to form EGS, where a fluid, typically water or brine, may then be circulated more easily than before. The artificially enhanced permeability needs to be high enough to reach flow rates that are commercially relevant for power production, depending on the subsurface working fluid. Larger permeability enhancements are required for water or brine than for CO_2, as the latter can utilize lower temperatures and lower permeabilities for economic geothermal power generation, due to its higher energy conversion efficiency (Brown, 2000; Pruess, 2006, 2007; Randolph and Saar, 2011a, 2011b; Adams et al., 2014, 2015; Garapati et al., 2015; Buscheck, 2016). Moreover, fluid flow should occur within a large number of permeable fracture pathways that sweep a large surface area of the rock, thereby providing longevity to the system and avoiding early thermal breakthrough, such as occurred at the Rosemanowes Project (Parker. 1999) and the Hijiori Project (Tenma et al., 2008). The construction of such systems (i.e., an artificial reservoir with sufficient permeability for energy extraction) is one of the key research challenges for unlocking the large potential of deep geothermal energy. The creation of a subsurface heat-exchanger between the boreholes in the low permeability rock mass typically involves hydraulic stimulation, i.e., fluid injections, during which the pore pressure is raised in the rock mass leading to the enhancements of permeability of natural fractures and faults, and perhaps the creation of new fractures.

Hydraulic stimulation is inevitably accompanied by induced seismicity (e.g., Zoback and Harjes, 1997; Evans et al., 2005a; Davis et al., 2013, Bao and Eaton, 2016), because the slip triggered by the elevated pore pressure arising from injections may be sufficiently rapid to generate seismic waves. In shale gas- and EGS-related stimulations, clouds of small induced (micro-)seismic events are important monitoring tools for delineating the location, where rock mass volume is undergoing stimulation (e.g., Wohlhard et al., 2006). Unfortunately, seismic events induced by the stimulation injections may be large enough to be felt by local populations and even to cause infrastructure damage (e.g., in Basel, 2006; Giardini, 2009). In the past few years, induced seismicity has been recognized as a significant challenge to the widespread deployment of EGS technology. From a reservoir engineering perspective, EGS faces two competing but interrelated issues: 1) rock mass permeability must be significantly enhanced by several orders of magnitude within a sufficiently large volume to enable sustainable heat extraction over many years (i.e., 20 – 30 years) while 2) keeping the associated induced seismicity below a hazardous level (Evans et al. 2014). Designing reservoir stimulation practices that optimize permeability creation and minimize induced seismicity requires a greatly improved understanding of the seismo-hydro-mechanical (SHM) response of the target rock mass volume. Seismo-hydro-mechanical processes relevant for stimulation involve 1) HM-coupled fluid flow and pressure propagation, 2) transient pressure- and permanent slip-dependent permeability changes, 3) fracture formation and interaction with pre-existing structures, 4) rock mass deformation around the stimulated volume due to fault slip, failure processes and poroelastic effects, and 5) the transition from aseismic to seismic slip.

In 2017, a decameter-scale, in-situ, stimulation and circulation (ISC) experiment was conducted at the Grimsel Test Site (GTS), Switzerland, with the objective of improving our understanding of the aforementioned HM-coupled processes in a moderately fractured crystalline rock mass. The ISC experiment activities aim to support the development of EGS technology by 1) advancing the understanding of fundamental processes that occur within the rock mass in response to relatively large-volume fluid injections at high pressures, 2) improving the ability to estimate and model induced seismic hazard and risk, 3) assessing the potential of different injection protocols to keep seismic event magnitudes below an acceptable threshold, 4) developing novel monitoring and imaging techniques for pressure, temperature, stress, strain and displacement as well as geophysical methods such as ground-penetrating radar (GPR), passive and active seismics and 5) generating a high-quality benchmark dataset that facilitates the development and validation of numerical modelling tools.

This paper presents a literature review that highlights key research gaps concerning hydraulic reservoir stimulation, and discusses which of the aforementioned research questions can be addressed in our decameter underground stimulation experiment. We then provide an overview of the ISC project that describes the geological site conditions, the different project phases and the monitoring program.

2 Literature review

2.1 Stimulation by hydraulic shearing

The concept of mining heat from hot, low permeability rock at great depth was first proposed at Los Alamos National Labs in the 1970s and was called Hot Dry Rock system (Brown et al., 2012). They initially envisioned creating a reservoir by applying oil and gas reservoir hydrofracture technology to build a heat exchanger between two boreholes. Subsequent field tests have demonstrated that hydraulic stimulation injections are effective in enhancing the permeability of a rock mass by several orders of magnitude by producing irreversible fracture opening, whilst also increasing the connectivity of the fracture network (Kaieda et al., 2005, Evans et al., 2005b; Häring et al., 2008). Two different 'end-member' mechanisms commonly appear in discussions of permeability creation processes through hydraulic injections: 1) hydraulic fracturing as the initiation and propagation of new tensile fractures and 2) hydraulic shearing, i.e., the reactivation of existing discontinuities in shear with associated irreversible dilation that is often referred to as the self-propping mechanism. Hydraulic shearing is of particular relevance for EGS as it has been shown that slip along fractures can generate a permeability increase by up to 2-3 orders of magnitude (Jupe et al., 1992, Evans et al., 2005a; Häring et al., 2008). If the rock mass in the reservoir is stressed to a critical level (e.g., Byerlee 1978), then a relatively small reduction of effective normal stress would be sufficient to cause shearing along pre-existing discontinuities that are optimally-oriented for failure (Hubbert and Rubey, 1959; Rayleigh et al., 1976; Zoback and Harjes 1997; Evans et al., 1999; Evans, 2005). Thus, shearing and the associated permeability enhancement can occur at large distances from the injection point, even though the causal pressure increases may be low (Evans et al., 1999; Saar and Manga, 2003; Husen et al., 2007). In contrast, hydraulic fracture initiation and propagation (i.e., the original concept of EGS to connect two boreholes) requires high pressures exceeding the minimum principal stress to propagate hydro-fractures away from the wellbore. The high pressure in the fracture may interact with natural fractures and stimulate them, leading to leak-off (i.e., the extent of hydro-fractures is influenced by pressure losses and the existence of pre-existing fractures). Therefore, hydraulic fracturing is often only considered relevant in the near-field of a wellbore, where it improves the linkage between the borehole and the natural fracture system. Rutledge et al., (2004) showed that shear activation of existing fractures and creation of new fractures can occur concomitantly, dependent on the in-situ stress conditions, injection pressure, initial fracture transmissivity, fracture network connectivity and fracture orientation (e.g., McClure and Horne, 2014). Regardless of which process is dominant, the direction of reservoir growth, and therefore, the geometry of the stimulated volume, depends to a considerable degree on the in-situ stress gradient, stress orientation and the natural fracture network.

Pressurized fractures may open due to a reversible compliant response to pressure (Rutqvist 1995; Rutqvist and Stephansson 2003; Evans and Meier, 2003), or due to largely irreversible shear dilation (Lee and Cho 2002; Rahman et al., 2002). As a consequence of the coupling between pressure, fracture compliance and permanent fracture aperture changes, the pressure field does not propagate through the reservoir as a linear diffusive field, but rather as a pressure front (Murphy et al., 2004). The fracture normal and shear dilation that occurs in response to elevated fluid pressure thus has a major influence on the magnitude and profile of the propagating pressure perturbation in the rock mass during hydraulic stimulations (Evans et al., 1999; Hummel and Müller, 2009). As a consequence, fracture compliance and normal/shear dilation characteristics have an impact on the size and geometry of the reservoir created during hydraulic stimulation.

Although the aforementioned processes are conceptually well understood, the quantification and detailed understanding required for designing stimulations and truly engineering geothermal reservoirs are insufficient. There remains considerable uncertainty as to how the above processes interact, and what rock mass characteristics and injection metrics control the dominant mechanisms (Evans et al, 2005a; Jung 2013). Thermo-hydro-mechanically coupled numerical models have become widely used for analysing relevant aspects of reservoir stimulation in retrospective (e.g., Baujard and Bruel, 2006; Rutqvist and Oldenburg 2008; Baisch et al., 2010; Gischig and Wiemer, 2013) or as prospective tools for predicting reservoir behaviour or alternative stimulation strategies (e.g., McClure and Horne 2011; Zang et al., 2013; Gischig et al., 2014; McClure 2015; Yoon et al., 2015). The fact that such numerical models must be parameterized from sparse quantitative field-scale data is a major limitation of all those studies. In the following we present an overview of the experimental observations of hydro-mechanical coupling that are relevant to the parameterization of numerical models. These stem from reservoir-scale (i.e., hectometre) stimulation operations, such as in EGS demonstration projects or oil and gas reservoirs, intermediate-scale (i.e., decametre) in-situ-experiments, and small-scale laboratory experiments.

2.1.1 Reservoir-scale experiments

The paucity of high-quality data on the stimulation process from reservoir-scale projects is largely a result of the considerable depth of typical geothermal resources (e.g., several kilometres), which prohibits the observation of hydro-mechanical processes from instrumentation installed within the reservoir. In the geothermal domain, such projects constitute expensive experiments and thus are relatively few in number, whereas, in the oil and gas domain, where hydrofracture operations are frequent and routine, the data tend to be proprietary. Nevertheless, some notable datasets have been acquired for deep brine injection projects (Ake et al., 2005; Block et al., 2015), deep scientific drilling projects such as the German KTB project (Zoback and Harjes 1997; Emmermann and Lauterjung 1997; Jost et al., 1998; Baisch and Harjes 2003), hydraulic fracturing for oil & gas production enhancement (Warpinski 2009; Das and Zoback 2011; Dusseault et al., 2011; Pettitt et al., 2011; Vermylen and Zoback 2011; Boroumand and Eaton 2012; van der Baan et al., 2013; Bao and Eaton 2016;), and during the stimulation of deep geothermal boreholes (Parker, 1989; Jupe et al., 1992; Cornet & Scotti, 1993; Tezuka & Niitsuma, 2000; Asanuma et al., 2005; Evans et al., 2005a; Häring et al., 2008; Brown et al., 2012; Baisch et al., 2015;). Well-documented hydraulic stimulation datasets generally include microseismic observations as well as injection pressures and flow rates and occasionally, tilt monitoring (Evans, 1983; Warpinski et al., 1997). Although much information can be gained from these datasets, including imaging of microseismic structures (Niitsuma et al. 1999; Maxwell, 2014), energy balance between injected fluids and seismic energy release (Boroumand and Eaton 2012; Zoback et al., 2012; Warpinski et al., 2013), and source mechanisms (Jupe et al., 1992; Deichmann and Ernst, 2009; Warpinski and Du 2010; Horálek et al, 2010), the constraints placed on the processes are insufficient to resolve details of the hydro-mechanical processes that underpin permeability enhancement, flow-path linkage, channelling, or the interaction with natural fractures. Many of these processes possibly also depend on rock type. For instance, case studies analysed by Evans et al., (2012) support the notion that injection into sedimentary rock tends to be less seismogenic than in crystalline rock. Moreover, it is likely that a significant part of the permeability creation processes take place in an aseismic manner (Cornet et al., 1997; Evans et al., 1998; Guglielmi et al., 2015b; Zoback et al., 2012), implying that seismic monitoring may only illuminate part of the stimulated rock volume. In many deep hydraulic stimulation projects the rock mass is only accessed by one or at most a few boreholes, and the structural and geological models of the reservoir are not well defined. In general, the displacements on fractures arising from the injection can only be directly measured where they intersect the boreholes, and deformation occurring within the rock mass is poorly resolved.

Despite limitations in reservoir characterization and monitoring, significant insights into the stimulation process can be gleaned from the experience from the EGS projects that have been conducted to date. Two examples in crystalline rock are studies of stimulation-induced fault slip and changes of flow conditions in the fracture network associated with the permeability creation processes at the Soultz-sous-forêt (Cornet et al., 1997; Evans et al., 2005b) and the Basel EGS projects (Häring et al., 2008). At both sites, it has been shown that permeability in the near-wellbore region increased by 2-3 orders of magnitude. At Basel, a single initially-impermeable fracture has been shown to take at least 41% of the flow during the 30 l/s injection stage (Evans and Sikaneta, 2013), whereas at Soultz-sous-forêt, the stimulation of the 3.5 km deep reservoir served to enhance the injectivity of a number of naturally-permeable fractures (Evans et al., 2005b). These fractures tended to be optimally oriented for fault slip, as also found elsewhere by Barton et al. (1995, 1998) and Hickman et al. (1998). At Soultz-sous-forêt, it was possible to estimate stimulation-induced slip and normal opening of fractures that cut the borehole by comparing pre- and post-stimulation acoustic televiewer logs (Cornet et al., 1997; Evans et al., 2005). Shearing of fractures was also proposed as the predominant mechanism of permeability enhancement in granite at the Fjällbacka site in Sweden, by Jupe et al. (1992), based upon focal mechanism analysis. The above observations provide evidence of a link between shearing and permeability changes.

An additional, important lesson from deep stimulation projects is that the stress conditions in reservoirs may be strongly heterogeneous, and that this influences the flow field (e.g., Hickman et al, 2000). For instance, profiles of horizontal stress orientation defined by wellbore failure observations commonly show significant fluctuations whose amplitude varies systematically with scale (Shamir and Zoback, 1992; Valley and Evans 2009; Blake and Davatzes, 2011), even though that may have an average trend consistent with the tectonic stress field. Strong deviations may occur in the vicinity of faults, indicating past fault slip and complex fault zone architecture (Valley and Evans, 2010; Hickman et al., 2000). Similarly, the hydro-mechanical properties of faults depend on the fault architecture, which itself depends on lithology and the damage history accumulated over geological time (Caine et al., 2006, Faulkner and Rutter 2008; Guglielmi et al., 2008, Faulkner et al., 2010, Jeanne et al., 2012). Within a fault zone, permeability and compliance contrasts can vary by several orders of magnitude (Guglielmi et al., 2008), thus complicating the predictability of hydro-mechanical responses to stimulations. In some EGS projects, it was observed that the hydraulic communication between injection and production boreholes may be unsatisfactory for efficient exchange of heat, either because of high flow impedance, such as in granite rock at Ogachi, Japan, (Kaieda et al., 2005), or because of flow channelling, as inferred from early thermal drawdown in granitic rock at Rosemanowes, UK (Nicol and Robinson, 1990), and in granodiorite at Hijiori, Japan (Tenma et al., 2008).

2.1.2 Laboratory-scale experiments

On the laboratory-scale, considerable effort has been devoted to experiments that address the role of effective stress changes on normal fracture opening and closure, shear dilatancy and related permeability changes (Goodman 1974; Bandis et al., 1983; Yeo et al., 1998; Esaki et al., 1999; Gentier et al., 2000; Olson and Barton, 2001; Samuelson et al., 2009). These experiments have demonstrated that the relationships between fluid pressure change, fracture opening and flow within rough natural fractures are strongly non-linear. Even though significant progress has been made on defining permeability changes during normal opening and shear slip on the laboratory scale, the non-linear relationships between fracture opening, changes in effective normal stress, shearing, and the resulting permeability are yet not well constrained (Esaki et al., 1991; Olsson et al., 2001, Vogler et al., 2015). One common approach is to represent the fracture as two parallel plates whose separation, the hydraulic aperture, gives the same flow rate per unit pressure gradient as would apply for the natural fracture. For parallel plates and laminar flow, the flow rate per unit pressure gradient is proportional to the cube of hydraulic aperture. However, for rough-walled fractures, the hydraulic aperture, a_h, is generally only a fraction of the mean mechanical aperture, a_m (i.e., the mean separation of two surfaces), the fraction tending to decrease with smaller apertures, although the precise relationship is difficult to derive from fracture geometry alone (Esaki et al., 1999; Olsson and Barton 2001; Vogler et al., 2015). At larger mechanical apertures, limited evidence suggests that an incremental form of the cubic law might hold such that changes in mechanical aperture give rise to equal changes in hydraulic aperture, at least for normal loading (e.g., Schrauf and Evans, 1986; Evans et al. 1992; Chen et al., 2000). For shear-induced dilation, an additional complication arises from channel clogging due to gouge production (e.g., Lee et al., 2002). Particle transport through fluid flow (Candela et al., 2014) and mineralogy (Fang et al., 2017) may additionally influence permeability changes in a complex manner. Deviations from the cubic law also occur when flow becomes non-laminar, which tends to occur at high flow velocities (Kohl et al., 1997), or at feed points in boreholes (e.g., Hogarth et al., 2013; Houben, 2015).

Dilatancy associated with shearing is often expressed in terms of a dilation angle, which is a property describing the relationship between mean mechanical aperture and slip. Dilation angle depends on the fracture surface characteristics, the effective normal stress and the amount of slip. Particularly important within the stimulation context is the dependence of dilation on effective normal stress, the dilation angle tending to decrease at higher effective normal stress, in large part because shorter wavelength asperities are sheared off (Evans et al., 1999). Thus, shearing-induced dilation is likely to be more effective at low effective normal stress, such as in the near field of the injection where fluid pressures are relatively high. Clearly, insights from laboratory experiments into the relationships describing fracture dilation and permeability changes are important for understanding field observations in EGS reservoirs (e.g., Robinson and Brown; 1990; Elsworth et al., 2016; Fang et al., 2018), and also for parametrizing numerical models.

2.1.3 Intermediate-scale experiments

In-situ experiments at the intermediate-scale (i.e., decameter-scale) serve as a vital bridge between laboratory and reservoir scales. As such, they can contribute to an improved understanding of reservoir behaviour during stimulation, and to enable up-scaling of hydro-mechanical information obtained from laboratory experiments (Jung, 1989; Martin et al., 1990; Rudquist, 1995; Schweisinger et al., 1997; Cornet et al., 2003; Murdoch et al., 2004, Cappa et al., 2006; Derode et al., 2013; Guglielmi et al., 2014; 2015). Much experience has been gained from stress testing using the hydraulic methods of hydro-fracturing (HF), hydraulic testing of pre-existing fractures (HTPF) (Haimson and Cornet, 2003), and hydro-jacking (Evans and Meier, 1995; Rutqvist and Stephansson, 1996). Hydraulic tests have been commonly used to quantify pressure-sensitive permeability changes (Louis et al., 1977), and normal stiffness in natural fractures or faults (Rutqvist et al., 1998). Evans and Wyatt (1984) estimated the closure of a fracture zone from observed surface deformations induced by drilling-related drainage of fluid pressure within the structure. Similarly, Gale (1975), Jung (1989), Martin et al. (1990), Guglielmi et al (2006), and Schweisinger et al. (2009) used borehole caliper sondes to monitor changes in fracture aperture and pressure during hydraulic jacking tests. The resulting displacements and the flow and pressure responses allowed relationships between mechanical and hydraulic aperture changes to be established and helped to constrain the fracture/fault normal compliance at larger scales.

Irreversible permeability increases arising from slip-induced dilation of natural fractures are particularly relevant for stimulation of EGS and hydrocarbon reservoirs. To study the phenomenon in-situ, Guglielmi et al. (2014) developed a novel double packer system (SIMFIP) that allows the simultaneous measurement of pressure, flow rates and 3-dimensional relative displacements occurring across a fracture isolated within the interval in response to injection. The device was successful in reactivating a fault zone in a limestone formation in Southeast France (Derode et al., 2013; Guglielmi, et al., 2015). Pressure, injection rate and 3D displacements in the SIMFIP interval were measured, together with microseismic activity, tilt and fluid pressure in the vicinity of the injection borehole. The dataset is unique, and provided quantitative insights into the relationships between (i) fault dislocation including shear and permeability changes, (ii) fault normal compliance and static friction, and (iii) slip velocities and magnitudes and their relation to aseismic and seismic slip. Recently, a similar experiment was conducted in a series of interacting complex fault zones in shale (Guglielmi et al., 2015). Distributed pore pressure and strain sensors across the faults allowed the evolution of the pressurized and slipped areas to be constrained, which was not previously possible. Such experiments provide a useful methodology for advancing our understanding of the hydro-mechanical coupled processes in complex faults.

2.2 Stimulation by hydraulic fracturing

Experience gained from large scale stimulation of EGS reservoirs in crystalline rock suggests that hydraulic shearing is the dominant mechanism for permeability creation, at least several tens of meters distance from the injection point (e.g. Evans, 2014). However, the initiation and propagation of hydraulic fractures may be an important mechanism in the near field of the wellbore to connect the wellbore to the pre-existing fracture network in the reservoir (Cornet and Jones, 1994). Considerable effort has been devoted to understand the initiation and propagation of hydraulic fractures on both the laboratory and intermediate field scale.

2.2.1 Laboratory scale hydraulic fracturing experiments

Many well-controlled, small-scale laboratory experiments on hydrofracture are documented in the literature (Jaeger 1963; Zoback et al., 1977; Warpinski et al., 1982; Bruno and Nakagawa 1991; Johnson and Cleary 1991; Song et al., 2001; Jeffrey and Bunger 2007; Bunger et al., 2011). For such experiments, samples of various shapes (e.g., hollow cylinders and perforated prisms) are loaded along their boundaries and the internal fluid pressure is increased until a hydraulic fracture initiates and propagates. For some tests, transparent material like polymethylmethacrylate (PMMA) were used to image fracture growth. Some experimental setups include multi-material "sandwiches" to study the effect of stress contrast on hydraulic fracture containment (Jeffrey and Bunger 2007; Warpinski et al., 1982). Others study the interaction of propagating hydrofractures with pre-existing fractures (Zoback et al., 1977; Meng, 2011; Hampton et al, 2015) or rock textures (Ishida 2001; Chitrala et al., 2010), the impact of injection fluids with different viscosities (Bennour et al., 2015) or the role of stress anisotropy (Doe and Boyce, 1989) on the geometry and orientation of generated fractures, or the interaction between multiple fractures (Bunger et al., 2011). These laboratory studies provide important results relevant for EGS. For instance, in the common situation where a family of natural fractures in not normal to the minimum principal stress, injections with high viscosity fluids (viscosity dominated regime) may help maintain tensile fracture propagation normal to the minimum principal stress despite the presence of cross-cutting fractures (Zoback et al., 1977), whereas low viscosity fluids (toughness dominated regime) such as water will promote leak-off into the cross-cutting natural fractures, whose permeability may be increased by shear (Rutledge et al, 2003). This leak-off will tend to limit hydrofracture propagation. Laboratory studies also give insights into the influence of shear stress shadow and transfer on hydraulic fracture growth (Bunger et al., 2011). Laboratory tests have also been essential for providing well-controlled fracture initiation and propagation datasets to benchmark hydraulic fracture simulation codes (Bunger et al., 2007).

2.2.2 Intermediate scale hydraulic fracturing experiments

Intermediate scale experiments have been performed to study initiation and propagation of hydraulic fractures. Typically, they are conducted from boreholes drilled from excavations to facilitate dense near-field instrumentation and secure good experimental control. An early example is the series of experiments that took place at the Nevada Test Site in soft, bedded volcanic tuff with high porosity and high permeability (Warpinski, 1985; Warren and Smith, 1985). The pressure, flow and fracture aperture were monitored during the experiments, and the fractures were mined back at the end of the experiments. The mine back revealed that stress contrasts were the predominant influence on hydraulic fracture containment, and that the fractures consisted of multiple fracture strands and thus differed significantly from simple shapes assumed in theoretical studies. This complexity of the fracture shape impacts the flow and pressure distribution within the propagating hydraulic fractures. Another notable series of in-situ tests on hydraulic fracture propagation within the context of coal-seam mining and block cave mine preconditioning have been performed by the hydraulic fracture group of CSIRO (Chacón et al., 2004; Jeffrey et al., 1993; 1992, 2009; Jeffrey and Settari 1995; van As et al., 2004; van As and Jeffrey 2002, 2000). The block cave mining experiments were performed in hard rock media and thus are the more relevant to EGS. Those conducted in the quartz monzonite porphyries at the Northparkes mine in Australia are probably the most detailed and densely instrumented tests executed to date, and included tiltmeter monitoring, a micro-seismic network, and pore pressure sensors as well as detailed rock mass and stress characterization (Jeffrey et al., 2009). Hydrofractures were formed with water and cross-linked gels, with coloured plastic proppants added in order to facilitate their identification once the test volume was mined back. The mapped trajectories of the hydraulic fractures exhibited complex geometries, sometimes with multiple branching and crossing of joints, veins and shear zones, with and without offset. Sub-parallel propped sections accounted for 10 to 15% of the total fracture extent, which microseismic activity indicated was more than 40 m from the injection point. The results demonstrate that the geometry of the fractures is much more complex than typically obtained in small scale laboratory experiments in a homogeneous material and uniform stress field. The complexity close to the injection point is controlled by the near-well stress perturbation and the interaction with natural fractures and rock mass fabric.

Natural fractures have also a strong influence on the propagation of hydraulic fractures. The propagation regime (i.e., viscosity-dominated or toughness-dominated (Detournay, 2016)) can be controlled by the injection rate and injected fluid rheology and will have likely a strong influence on the interaction with natural fractures and the final complexity of the hydraulic fractures, although this has not been validated by in-situ experiment. Another relevant aspect that has not been investigated with in-situ tests is the problem of proppant transport and distribution within the created fractures. Indeed, in the case of hydraulic fractures, the self-propping mechanism, which results in a permanent aperture increase, is unlikely to be effective, and so proppant placement is necessary for insuring permanent permeability enhancement. Finally, the nature of the microseismicity generated by hydraulic fracturing is not adequately understood. Moment tensor analyses can offer insight into the nature of the failure in a microseismic event (Warpinski and Du, 2010; Eyre and van der Baan, 2015). For example, they can help resolve whether the seismic radiation is primarily generated by shear on pre-existing fractures that are intersected by the propagating fracture, with relatively little energy generated by the advancing mode 1 tip of the hydraulic fracture (Sileny et al, 2009; Horálek et al, 2010; Rutledge et al., 2004).

2.3 Rock mass deformation and stress interaction

Injection of fluid into a rock mass invariably leads to deformation of the surrounding rock mass due to poroelasticity (Biot 1941) or slip-related stress changes (McClure and Horne 2014). Numerical studies have suggested that stress interaction between adjacent fractures can have a significant impact on the stimulation results (e.g., Preisig et al., 2015; Gischig and Preisig 2015). In most reservoir stimulations, the microseismic clouds exhibit an oblate shape, due primarily to the interaction between the strongly anisotropic stress field with the natural fracture population. This tendency to form an oblate ellipsoidal shape instead of a sphere may also be promoted by stress transfer from slipped fractures which tends to inhibit slip on neighbouring fractures (Gischig and Preisig 2015). Schoenball et al. (2012) and Catalli et al. (2013) have demonstrated that induced earthquakes preferably occur where stress changes generated by preceding nearby earthquakes render the local stress field to be more favourable for slip. Similar effects have been observed for natural earthquakes (Stein 1999). The effect becomes more important during stimulation as time goes on, especially at the margin of the seismicity cloud. Direct observation of deformation associated with fluid injection has been observed in several intermediate-scale in-situ experiments. Evans and Holzhausen (1983) report several case histories of using tiltmeter arrays to observe ground deformation above high pressure hydraulic fracturing treatments. The results show clear evidence of self-propping of the induced fractures. van As et al. (2004). Jeffrey et al (2009) used a tiltmeter array to monitor a hydrofracturing treatment at the Northparkes mine in Australia. The pattern of tilting indicated the induced fracture was sub-horizontal, which was confirmed by excavating the fracture traces. Evans and Wyatt (1984) modelled strains and tilts occurring around a well during air drilling and found the deformation was due to opening of a pre-existing fracture zone in response to fluid pressure changes. Derode et al. (2013) observed tilts of 10^{-7}-10^{-6} radians some meters away from small volume injections into a fault in limestone. In contrast, Cornet and Deroches (1990) monitored surface tilts with a 6 instrument array during injections of up to 400 m^3 of slurries into granite at 750 m depth at the Le Mayet test site in France and report no resolved signal associated with the injections.

Rock mass deformation during stimulation injections necessarily leads to stress changes in the rock mass. Small but non-zero residual stress changes induced by hydraulic fracturing were measured using a stress cell by van As et al. (2004). Stress changes during injections are recognized as playing a potentially important role in determining the pattern of fracture and slip that develops during the injection (e.g., Preisig et al., 2015; Catalli et al, 2013).

2.4 Seismic and aseismic slip

A significant fraction of the slip that occurs on fractures within a reservoir undergoing stimulation may be aseismic, depending upon in-situ stress and geological conditions. That aseismic slip has occurred is often inferred indirectly from changes in the hydraulic characteristics of a reservoir without attendant micro-seismicity (Scotti and Cornet 1994; Evans, 1998). Direct detection of aseismic slip is difficult as it requires relative displacements across fractures to be resolved from borehole or near-field deformation measurements (e.g., Maury 1994; Cornet et al., 1997, Evans et al., 2005b). For example, Cornet et al. (1997) compared borehole geometry from acoustic televiewer logs run before and after the 1993 stimulation at the Soultz-sous-forêt site and found that 2 cm of slip had apparently occurred across a fracture. The cumulative seismic moment of events in the neighbourhood of the fracture was insufficient to explain the observed slip magnitude, thereby suggesting a large portion of the slip had occurred aseismically. Indeed, almost all fracture zones that were hydraulically active during the stimulation showed evidence of shear and opening-mode dislocations of millimetres to centimetres (Evans et al., 2005b).

The transition from aseismic to seismic slip was directly observed by Guglielmi et al. (2015) during fluid injection into a well-instrumented fault in limestone in a rock laboratory at 280 m depth. Some 70% of a 20-fold permeability increase occurred during the initial aseismic slip period. The transition to seismic slip coincided with reduced dilation, and the inference that slip zone area exceeded the pressurized area, suggesting the events themselves lay outside the pressurized zone. Modelling the observed slip as occurring on a circular fracture with total stress drop gave a radius of 37 m and a moment release of 65e9 Nm, far larger than the estimated seismic moment release of the order of 1e6 Nm, again indicating most slip was aseismic. Guglielmi et al. (2015) concluded that the aseismic behaviour is due to an overall rate-strengthening behaviour of the gauge filled fault and seismicity occurs due to local frictional heterogeneity and rate-softening behaviour. These results are consistent with laboratory experiments performed by Marone and Scholz (1988) on fault gauge which suggest that slip at low effective normal stresses (as anticipated in the near field of a high-pressure injection) and within thick gouge layers tends to be stable (aseismic).

Apart from these observations, aseismic slip has been mostly discussed from the perspectives of semi-analytical or numerical models. Garagash and Germanovic (2012) used a slip-weakening model to show that aseismic slip depends on the stress conditions and injection pressure. Zoback et al. (2012) used McClure's (2012) rate-and-state friction model to show that aseismic slip becomes more prominent for stress states farther from the failure limit. Using the same model, Gischig (2015) demonstrated that slip velocity depends on fault orientation in a given stress field. For non-optimally oriented faults, aseismic slip becomes more prominent and the seismicity is less pronounced for lower slip velocities and shorter rupture propagation distances. These model results suggest that aseismic slip and low slip velocities may be promoted by avoiding the stimulation of optimally oriented critically-stressed faults. Clearly, a more detailed understanding of the conditions that result in aseismic slip may be a basis for less hazardous stimulations.

2.5 Induced seismicity

Keeping induced seismicity at levels that are not damaging or disturbing to the population continues to be a major objective for EGS (Giardini, 2009; Bachmann et al., 2011; Majer et al., 2012; Evans et al., 2012) and other underground engineering projects (oil and gas extraction, liquid waste disposal, gas and CO_2 storage). Man-made earthquakes are not a new phenomenon (Healy et al. (1968), McGarr, 1976; Pine et al., 1987; Nicholson and Wesson, 1990, Gupta, 2003). However, the occurrence of several well-reported felt events near major population centres has served to focus attention on the problem (Giardini, 2009; Ellsworth 2013; Davies et al., 2013; Huw et al., 2014; Bao and Eaton, 2016). Some even led to infrastructure damage, such as followed the Mw5.7 event in Oklahoma, USA (Keranen et al., 2013), or the suspension of the projects (e.g., the geothermal projects at Basel (Häring et al., 2008) and St. Gallen (Edwards et al., 2014) in Switzerland. As a consequence, a substantial research effort has been initiated to understand the processes that underlie induced seismicity. Examples are the numerous studies that have been performed using the high-quality seismic dataset collected during the Basel EGS experiment. Dyer et al. (2010), Kraft and Deichmann (2014) and Deichmann et al. (2014) analysed waveforms of the seismicity to determine reliable source locations. Terekawa et al. (2013) used an extended catalogue of the focal mechanism solutions of Deichmann and Ernst (2009) to estimate the stress field at Basel and to infer the pore pressure increase required to trigger the events. Goertz-Allmann et al. (2011) determined stress drop for the Basel seismicity and found higher stress drops at the margin of the seismic cloud than close to the injection borehole. A similar dependency for Gutenberg-Richter b-values was found by Bachmann et al. (2012) – lower b-values tended to occur at the margin of the seismicity cloud and at later injection times.

There are numerous analyses of induced seismicity at other EGS sites. Pearson (1981) and Phillips et al (1997) analysed microseismicity generated during the stimulation of the 2930 m deep 'large Phase 1' and the 3'460 m deep Phase 2 reservoirs respectively at the Fenton Hill EGS site, New Mexico. Bachelor et al. (1983) and Baria and Green (1986) summarize microseismicity observed during the stimulation injections into the Phase 2a and 2b reservoirs at Rosemanowes in Cornwall, UK. Tezuka and Niitsuma (2000) examined clusters of microseismic events generated during the stimulation of the 2200 m deep reservoir at the Hijiori EGS site in Japan. Baisch et al. (2006, 2009, 2015) analysed data from different stages of the stimulation of the Habanero EGS reservoir in the Cooper Basin, Australia. Calò et al. (2011) used microseismicity generated during the stimulation of the 5 km deep EGS reservoir at Soultz-sous-forêt to perform time-lapse P-wave tomography to infer pore pressure migration during injection. Various authors also explored the vast induced seismicity dataset of >500'000 events recorded since the 1960s at the Geysers geothermal site where recently also an EGS demonstration stimulation has been performed (Garcia et al., 2012; Jeanne et al., 2014). The observed seismicity was partly related to injections (Jeanne et al., 2015) and thermo-elastic stress changes (Rutqvsit and Oldenburg, 2008). Here, local variability in the stress field (Martínez-Garzón et al., 2013) and volumetric source components (Martínez-Garzón et al., 2017) were inferred from detailed analysis of injection-induced seismicity.

Another major focus of induced seismicity research has been the development of hazard assessment tools for injection related seismicity. The primary goal of these efforts is to develop a dynamic, probabilistic and data-driven traffic light system that can provide real-time hazard estimates during injections (Karvounis et al., 2014; Kiraly et al, 2016), as opposed to the traditional, static traffic light system (Bommer et al., 2006). Bachmann et al. (2011) and Mena et al. (2013) developed several statistical models and tested them in pseudo-prospective manner using the Basel seismicity dataset. More complex models including physical considerations and stochastic processes (so-called hybrid-models) were developed to include information on the reservoir behaviour and from the spatio-temporal evolution of seismicity (Goertz-Allmann and Wiemer, 2013; Gischig and Wiemer, 2013; Kiràly et al., 2016). Mignan et al. (2015) evaluated reported insurance claims arising from the Basel induced seismicity in order to infer procedures for evaluating risk based on induced seismic hazard estimates.

The Gutenberg-Richter b-value, which describes the reduction in the frequency of occurrence of events with increasing earthquake magnitude, plays a key role in induced seismic hazard analysis. Schorlemmer et al. (2005) examined the b-values of earthquakes in different stress regimes and found lower values correlated with areas of higher differential stress. Similar trends have been reported for induced seismicity (Bachmann et al., 2012), but also in tectonic earthquakes (Tormann et al., 2014; Torman et al., 2015; Spada et al., 2013) and laboratory experiments (Amitrano 2003; Goebel et al., 2012). Thus, it was hypothesized that b-values are related to local stress conditions (Scholz, 2015), or - in the context of induced earthquakes – to a combination of pressure and stress conditions. Considering standard scaling laws between magnitudes and earthquake source dimensions (i.e., slip and slipped area), it has to be expected that seismicity with high b-values may have an indirect but strong impact on permeability enhancement (Gischig et al., 2014). However, these observations have so far only been qualitatively established, as the absolute stress state within the rock volume that hosts the seismicity whose b-value is estimated has not been quantitatively determined.

Whilst the hazard associated with induced seismicity is clearly an important factor for reservoir engineering, it should not be forgotten that the shearing of fractures and fracture zones, which is the source of the seismicity, is a key process in the irreversible permeability enhancement that is the objective of the stimulation injections. Furthermore, precise mapping of the 3-D distribution of events provides an indication of the direction of fluid pressure propagation and hence the geometry (i.e., size, shape, degree of anisotropy) of the distribution of permeability enhancement – information that is vital for drilling subsequent well (Niitsuma et al., 1999). Managing induced seismic hazard also requires considering the design of reservoir attributes such as size, system impedance, and heat exchanger properties that control system longevity (e.g., Gischig et al., 2014). Currently, few case studies consider both seismicity and the related changes that occurred in the reservoir (e.g., Evans et al., 2005a), and relatively few studies even report both permeability changes or well injectivity (e.g., Häring et al., 2008; Evans 2005b; Kaieda et al., 2005; Petty et al., 2013). More work is needed to quantitatively link the spatial, temporal or magnitude distribution of seismicity with the thermo-hydraulic-mechanical properties of the rock mass under stimulation conditions. We believe controlled experiments on the intermediate (in-situ test site) scale supported by laboratory-scale experiments could be key in making progress towards this end.

2.6 Open research questions in hydraulic stimulation research

Research on reservoir stimulation for deep geothermal energy exploitation has been largely performed through laboratory observations, large-scale projects, and numerical models. Observations of full-scale reservoir stimulations have yielded important observations. However, the difficulty in observing the processes occurring within the reservoir under stimulation conditions severely limits the understanding of the permeability creation processes in a way that aids future stimulation design.

Laboratory experiments are attractive because they are controllable and readily repeatable, but they suffer from two main limitations: 1) Upscaling results to the field-scale is affected by large uncertainties (Gale 1993). Although there is evidence that the roughness of fresh fracture surfaces obeys well-defined scaling over many orders of magnitude (Power and Tullis, 1991; Schmittbuhl et al., 1995), complications arise in upscaling the aperture distribution and hence permeability of two semi-mated rough surfaces due to the effects of damage and wear of the asperities during shearing and gouge formation (Amitrano and Schmittbuhl, 2002; Vogler et al, 2016). 2) Laboratory tests are typically performed on single fractures in relatively homogeneous materials and uniform stress conditions, which makes upscaling to structures with multiple fractures such as fracture zones challenging. Similarly, hydraulic fracture propagation behaviour is usually studied with homogenous rock samples under uniform stress, and this can lead to an over-simplistic fracture flow and/or hydraulic fracture propagation behaviour. In an EGS reservoir, for example, the stress may be heterogeneous on the meter to decametre-scale (Evans et al., 1999; Valley and Evans 2009; Blake and Davatzes, 2011), and the rock mass may contain various heterogeneities such as stiffness contrasts, fractures or faults (Ziegler et al., 2015).

Because of the large uncertainties in upscaling, many numerical studies make direct (i.e., not upscaled) use of laboratory results to parameterize HM-coupled models for EGS, because so few field-scale relationships are available (e.g., Rutqvist, 2011; McClure, 2012; Gischig et al., 2014). This impacts the reliability of the numerical simulation studies, because the descriptions of the processes and the input parameter values may be inappropriate for the scale of the simulation.

Clearly there is a need for field-scale hydraulic stimulation experiments that bridge the various scales, and are performed with the target rock mass equipped with a comprehensive monitoring system to capture details of the processes. Recently several intermediate-scale hydro-shearing and hydrofracturing experiments have been performed in a densely instrumented rock mass (i.e., Guglielmi et al., 2008, 2014 and 2015; Jeffrey et al., 2009). The hydro-shearing experiments by Guglielmi et al. (2008) have all been in sedimentary rock types at shallow depth. No such densely-instrumented experiments have been performed in fractured and faulted crystalline basement rocks faults, the target rocks for most EGS, where a variety of complex fault architectures and stress-fracture system configurations need to be investigated. The In-situ Stimulation and Circulation (ISC) experiment addresses these research gaps, with a focus on the following research questions (RQ):

[RQ 1] What is the relationship between pressure, effective stress, fracture aperture, slip, permeability and storativity (i.e., the hydro-mechanical coupled response of fractures)?

[RQ 2] How does the transient pressure field propagate in the reservoir during stimulation?

[RQ 3] How does the rock mass deform as a result of rock mass pressurization, fracture opening and/or slip?

[RQ 4] How does stress transfer inhibit or promote permeability enhancement and seismicity along neighbouring fractures?

[RQ 5] Can we quantify the transition between aseismic and seismic slip and the friction models (such as rate-and-state friction) describing slip evolution and induced seismicity?

[RQ 6] How do hydraulic fractures interact with pre-existing fractures and faults and how can the interaction be controlled?

[RQ 7] How does induced seismicity evolve along faults and fractures of different orientation?

[RQ 8] How does induced seismicity along stimulated faults compare to induced seismicity along newly created hydraulic fractures?

[RQ 9] Can we quantify the link between spatial, temporal and magnitude distribution of induced seismicity and HM coupled properties of fractures and faults?

3 The ISC experiment

The objective of the ISC experiment is to find answers to the above mentioned research questions by 1) stimulating a naturally fractured crystalline rock volume at the decameter scale that is exceptionally well characterized in terms of its structural, geomechanical, and hydraulic conditions and 2) providing a dense network of sensors within the test volume so as to establish a 3D data set at high spatial resolution that will yield detailed insight into geomechanical processes associated with induced micro-earthquakes, fracture shearing, permeability creation and fluid circulation. The experiment was planned and prepared during 2015 and 2016, and executed during two series of experiments in February and May 2017. We here give a general overview of the experiment site, the main concepts, and the design of the experiment, without detailing results that are to be published in future work.

3.1 The in-situ rock laboratory

The ISC experiment was performed at the Grimsel Test Site (GTS), near the Grimsel Pass in the Swiss Alps (Figure 1a). The GTS is owned by the National Cooperative for the Disposal of Radioactive Waste (NAGRA), and was developed to host in-situ experiments relevant to nuclear waste repository research. The facility consists of a complex of tunnels at a mean depth of 480 m that penetrate crystalline rock with well-documented structures. The rock type is considered representative for the Alpine crystalline basement that is a main target for EGS. The test site for the ISC experiment is located in the southern part of the GTS (marked in blue in Figure 1b) between a Tunnel that is called AU Tunnel in the west and the VE Tunnel in the east.

The rock at the GTS consists of Grimsel granodiorite and Central Aar granite. Both show an alpine foliation that strikes NE and dips steeply at ~77° towards SE. The moderately fractured rock mass is intersected by ductile and brittle shear zones, as well as brittle fractures and metabasic dykes. Within the ductile shear zones, numerous fractures that are commonly partially filled with gouge are present. Three shear zone orientations can be distinguished at the GTS (Keusen 1989). The S1 shear zones are parallel to the alpine foliation with an orientation of 142/77 (i.e., dip-direction/dip). The S2 shear zones are slightly younger than S1 and oriented with 157/75 (Wehrens, 2015). The youngest shear zone direction (so-called S3), have E-W strikes and southward dips (183/65), and often show evidence of dextral strike-slip movement.

3.2 Experimental Phases

The ISC experiment was divided into three phases (Figure 2). The *first phase* (2015-2016) was a pre-stimulation phase that aims to characterize the rock volume in terms of geological and structural conditions, the local stress state, hydraulic and thermal properties, and fracture connectivity, all of which is essential for the design of the experiment and the interpretation of experimental results. In addition, during the pre-stimulation phase, a monitoring system was established that allows capturing the seismo-hydro-mechanical response at high spatial and temporal resolution. The *second phase* (February – May 2017) - the main hydroshearing and hydrofracturing experiment - was concerned with enhancing the permeability of the rock mass with high pressure fluid injections. A *third and final phase* (June – December 2017), the post-stimulation phase, was dedicated to characterize the rock mass in great detail after stimulation to quantify changes in permeability, fracture connectivity and heat exchanger properties.

3.2.1 Pre-Stimulation Phase – Rock mass characterization and Instrumentation

3.2.1.1 Boreholes, rock mass characterization and geological model

The governing aspects for designing the instrumentation of the decameter-scale ISC experiment were 1) a detailed understanding of the geological settings in 3-dimensions (e.g., fracture and fault orientation and intersections, fracture density, etc.) 2) the in-situ state of stress, 3) the pre-stimulation hydraulic conditions, including the flow field, preferential fluid flow path ways and transmissivities, 4) the borehole sections used for stimulation, 5) the type of hydraulic injection (i.e., hydraulic shearing or hydraulic fracturing) and 6) anticipated quantities and spatial distributions of strain, tilt and pressure within the rock volume during stimulation.

During the pre-stimulation phase a series of 15 cored boreholes with a length between 18 and 50 m and diameters between 86 and 146 mm were drilled within or about the experimental volume (Figure 3). Three boreholes were dedicated to stress measurements (SBH), two to the stimulation injections (INJ), four to geophysical characterization and monitoring (GEO), three to strain and temperature measurements (FBS) and another three to pore pressure, strain and temperature measurements (PRP). The boreholes were characterized in terms of geologic structures, hydraulic properties and inter-borehole connectivity. Various geological (i.e., core logging), geophysical (i.e., optical televiewer logs, resistivity logs, full-wave sonic logs, ground penetrating radar (GPR) surveys and active seismic measurements between the injection boreholes) and single-hole and cross-hole hydraulic methods (i.e., packer tests such as pressure-pulse, constant-rate and constant head injection tests, oscillating pumping tests, and tracer tests using various solutes, DNA-encoded nanoparticles, and heat) were used. In addition to borehole-based characterization methods, the experimental rock volume was characterized using detailed tunnel maps, reflection GPR from the tunnel walls and active seismic data acquisition between the AU and VE tunnels (Figure 1b). The trajectories of the subsequent boreholes were chosen based on these preliminary geological and hydraulic data and simplified numerical HM-coupled models (i.e., using 3DEC, Itasca 2014) for stimulation scenarios that provided an estimate of the deformation field and pore pressure propagation along geological structures.

The joint interpretation of the all geophysical, geological and hydrogeological observations was used to constrain a 3D structural model of the experimental volume (Krietsch et al., 2017, Figure 4). The 3D model illustrates the intersection of the shear zones that were targeted during the ISC experiments within the experimental volume. S1 shear zones (numbered from north to south: S1.1 to S1.3) within the ISC test volume have similar orientations as the overall foliation in the rock mass. Two major meta-basic dykes (S3.1 and S3.2) up to 1 m thick with a spacing of 2 m crosscut the volume in east-west direction. These metabasic dykes form the boundary of a zone with a high fracture density and partly open fractures, which together with the dykes define the S3 shear zone. The majority of brittle fractures within and outside the S3 shear zone are oriented parallel to the boundaries of the sheared metabasic dykes, which strike E-W in the test volume. Very few fractures penetrate into the dykes.

3.2.1.2 Rock mass instrumentation

In addition to a detailed characterization of the test volume for the design and interpretation of the in-situ experiment, a dense sensor network was required to collect the necessary data at a sufficient spatial resolution that were needed to address the previously mentioned research questions (RQ1-9). This includes pore pressure monitoring, strain and tilt and micro-seismic monitoring. Instrumentation design was also governed by the types of hydraulic injection treatments that were performed in the ISC experiment, i.e., hydraulic shearing (pressurization and reactivation of natural fractures and faults) and hydraulic fracturing (i.e., initiation and propagation of new fractures).

Pore pressure, deformations and temperature

To address questions related to hydro-mechanics (RQ1), pressure propagation (RQ2) and interaction between pre-existing and hydraulic fractures (RQ6), four pressure monitoring boreholes (three PRP boreholes and SBH15.004; Figure 3) were instrumented at points where they cut relevant structures. The boreholes were drilled approximately normal to the strike of the main geological features (S1 and S3 shear zones). They were completed with cement and resin-grouted packer systems with fixed open pressure monitoring intervals that record the pressure within fracture zones or fault zones. Pressure was also recorded in the INJ borehole that was not used for stimulation (Figure 3) with a straddle packer system similar to the one used for high pressure fluid injections. The PRP boreholes were also equipped with pre-stressed distributed fibre optics (FO) cables for strain and temperature measurements. Strain recordings give information on the HM response to pressurization across pre-existing fractures (RQ1), and help to detect propagation of new fractures during hydrofracturing experiment (RQ6). Distributed temperature measurements were used during pre- and post-stimulation thermal tracer tests.

To address research questions related to rock mass deformations (RQ3-6), three boreholes (FBS16.001-3 in Figure 3) were equipped with both distributed and Fiber Bragg Grating (FBG) strain-sensing optical fibers that were grouted in place. One borehole (FBS16.001) is approximately normal to the strike of the main geological features and intersects both the S3 and S1 fault zones. Another borehole is parallel to the strike of the S3.1 fault and intersects the S1.1 fault (FBS16.002), and one is parallel to the S1.2 faults and intersects the S3 fault zone (FBS16.003). The FBG sensors record axial strain across borehole sections that span potentially active fractures or the ‘intact’ rock mass. Distributed strain-sensing optical fibers allow a dense spatial coverage and thus are more likely to observe the propagation and opening of a hydraulic fracture.

The borehole strain monitoring system was complemented with an array of 3 biaxial tiltmeters installed on the margins of the test volume along the VE tunnel near the S3 fault zone (Figure 3). The tilt sensors were mounted in shallow holes drilled into the tunnel floor and record horizontal tilt. Together, the tilt measurements and the longitudinal strain in the FO boreholes were capable to describe the deformation field around the stimulated rock volume and allowed constraining the characteristics of the stimulated fault zones (i.e., dimension, dislocation direction and magnitude, etc.).

Micro seismicity

Questions related to induced seismicity (RQ5, 7, 8) were tackled using a microseismic monitoring system, which consists of a sensor network with 14 piezosensors affixed to the tunnel walls, and 8 sensors that were pressed pneumatically against the borehole wall in the geophysical monitoring boreholes (GEO16.001 – 4, Figures 3 and 5). The uncalibrated piezosensors were complemented with calibrated accelerometers (as done by Kwiatek et al., 2011) at five locations on the tunnel surface to enable the calculation of absolute magnitudes. A real-time event detection, first arrival determination and location algorithm gave provisional event hypocentres.

The sensor network was also used to recorded periodic active seismic experiments. Highly reproducible sources (i.e., piezoelectric pulse sources in boreholes and hammers installed at the tunnel walls with pre-defined constant fall height, Figure 5) were triggered roughly every 10 minutes during the stimulation experiments with the goal of recording systematic changes in the waveform characteristics that allow inferring changes of seismic velocity, attenuation and scattering properties. Such measurements can give additional constraints on 3D pressure propagation and deformation characteristics (RQ1-4, 9).

3.3 Stimulation Phase

The stimulation experiments were performed in two experiment sequences: 1) In February 2017, six hydraulic shearing experiments were performed including high-pressure water injection into existing faults or fracture zones so as to reduce effective normal stress and trigger shearing. 2) In May 2017, six hydraulic fracturing experiments were conducted with high pressure injection into fracture-free borehole intervals so as to initiate and propagate hydraulic fractures.

Two 146 mm diameter, downwardly-inclined boreholes (INJ 1 and INJ 2 in Figure 3) were dedicated for the injections from packer-isolated intervals. For the stimulation operations, water or gel was injected into a 1-2 m interval in one borehole, and the second borehole was used to additionally monitor the fluid pressure response. The maximum injected volume for the stimulation at each interval was limited to about 1000 liters. This value was determined as part of a pre-experiment hazard and risk study (Gischig et al., 2016) and was found to be acceptable regarding the estimated likelihood of inducing seismic events that could be felt in the tunnels, as well as the disturbance to on-going experiments elsewhere in the GTS. We used standardized injection protocols for HS and HF (i.e., we did not test different injection strategies) so that the variability in the rock mass response arises from differences of local hydromechanical conditions as well as geological settings, and not from different injection strategies.

3.3.1 Hydroshearing experiments

The stimulation injections targeted natural fracture zones in the rock volume whose transmissivities ranges from 1e-7 to 1e-10 m^2/s. Each interval stimulation consisted of four cycles (Figure 6). The objective of the first cycle was to measure initial transmissivity and jacking pressure, and break down the interval. Initially (Cycle 1), pressure was increased in small steps until breakdown occurred, as evidenced by a disproportionate increase in flow rate. This first cycle allowed quantifying the initial injectivity. After venting, the test was repeated with refined pressure steps (Cycle 2) in a narrow range to identify the jacking pressure. After Cycle 2 the interval was shut-in to capture the pressure decline curve before the interval was vented. The purpose of the third cycle was to increase the extent of the stimulation away from the injection interval. For this purpose, a step-rate injection test with four or more steps was utilized. The interval was then shut-in and the pressure decline was monitored for 40 minutes before initiating venting for 30 minutes. The purpose of the fourth cycle was to determine post-stimulation interval transmissivity and jacking pressure for comparison with pre-stimulation values. Thus, a step-pressure test was conducted initially taking small pressure steps to define the low-pressure Darcy trend and the deviation from it defining the jacking pressure. Following this cycle, the interval was shut-in for 10 minutes before venting. An important aspect for the quantification of irreversible changes in the reservoir was to run acoustic televiewer logs across each interval before and after the stimulation to attempt to resolve any dislocation that may occur across the fractures in the interval.

3.3.2 Hydraulic fracturing experiment

The protocol for hydraulic fracturing tests in borehole intervals without natural fractures is shown in Figure 7. Each interval stimulation consisted of three cycles. First, the packed interval was tested with a pulse for integrity. The measured transmissivity in intact rock ranges from 1e-13 to 1e-14 m^2/s. The objective of the first cycle was to break down the formation (i.e., to initiate a hydraulic fracture) using small flow rates (i.e., around 5 l/min injections for 60 s). The second cycle aimed to propagate the hydraulic fracture away from the wellbore and connect to the pre-existing fracture network using progressively increasing flow rates (up to 100 l/min). A shut-in and venting period followed. Finally, the purpose of the third cycle was to quantify the final injectivity and jacking pressure using a pressure step injection similar to the pressure step injection considered for cycle 4 in the fault slip experiments. Both pure water and a gel (i.e., a Xanthan-water-salt-mixture with 0.025 weight percent of Xanthan and 0.1 weight percent of salt with a viscosity between 35 and 40 cPs) were used for fracture propagation. If gel was used, cycle 2 is extended with a flushing cycle (with water) after fracture propagation. The two injection fluids allowed investigating two different propagation regimes (i.e., toughness-dominated and viscous-dominated). A specific amount of salt was added to each injection fluid as a tracer, to investigate flow paths and dilution effects. Further, a cyclic injection sequence was included in the fracture propagation cycle to test as an alternative injection protocol as proposed by Zang et al. (2013). They proposed that using cyclic injection the same efficiency in fracture propagation can be reached, while the associated micro-seismic event release is limited and fracture branching is enhanced.

3.4 Post-Stimulation Phase

In the last experiment phase, the changes to the hydrology and rock mass properties that occurred because of each of the two stimulations phases (i.e., the hydraulic shearing and hydraulic fracturing phases) were investigated. Accordingly, after each phase, a characterization program was performed. The hydraulic properties of the rock mass were determined using single-hole and cross-hole hydraulic methods. Selected stimulation intervals were isolated with packers and then subjected to a variety of tests including pressure-pulse, constant-rate and constant head injection tests, oscillating pumping tests, and tracer tests using solute dyes, DNA-tagged nanoparticles and heat. In addition, single hole, cross-hole, and cross-tunnel active seismic and GPR measurements were conducted. Repeat geophysical borehole logs were run in both injection boreholes, including focused resistivity, and full-wave sonic.

4 Summary and Conclusion

The review of scientific research results showed that carefully analyzed data from large-scale experiments (i.e., EGS projects) and laboratory scale experiments provide a fundamental understanding of processes that underpin permeability creation and induced seismicity in EGS. The results from large-scale experiments suffer from accessibility and resolution, which does not permit to resolve the details of seismo-hydro-mechanical coupled processes associated with the stimulation process. Laboratory scale experiment provide a fundamentally improved understanding of these processes but suffer from scalability and test conditions that may lead to over-simplistic fracture flow and/or hydraulic fracture propagation behavior that is not representative for a heterogeneous reservoir. Intermediate-scale experiments can serve to bridge the gap between the laboratory and the large scale and may enable upscaling of results gained from small scale experiments. However, only few intermediate-scale hydro-shearing and hydro-fracturing experiments have recently been performed in a densely instrumented rock mass and no such measurements have been performed on faults in crystalline basement rocks.

We have provided here an overview of the intermediate scale hydroshearing and hydrofracturing experiment (i.e., ISC experiment) that was executed in 2017 in the naturally fractured and faulted crystalline rock mass at the Grimsel Test Site (Switzerland). It was designed to fill some of the key research gaps and thus contribute to a better understanding of seismo-hydro-mechanical processes associated with the creation of Enhanced Geothermal Systems. As this contribution is meant to only provide a literature review and an overview of our ISC experiment at the Grimsel Test Site, several other publications will provide more detailed descriptions and analyses of this intermediate-scale hydroshearing and hydrofracturing experiment.

5 Acknowledgment

The ISC is a project of the Deep Underground Laboratory at ETH Zurich, established by the Swiss Competence Center for Energy Research - Supply of Electricity (SCCER-SoE) with the support of the Swiss Commission for Technology and Innovation (CTI). Funding for the ISC project was provided by the ETH Foundation with grants from Shell and EWZ and by the Swiss Federal Office of Energy through a P&D grant. Hannes Krietsch is supported by SNF grant 200021_169178. The Grimsel Test Site is operated by Nagra, the National Cooperative for the Disposal of Radioactive Waste. We are indebted to Nagra for hosting the ISC experiment in their GTS facility and to the Nagra technical staff for onsite support. We also thank two anonymous reviewers for their valuable input.

6 References

Achtziger-Zupančič P., Loew S. and Mariéthoz G. (2017). A new global database to improve predictions of permeability distribution in crystalline rocks at site scale. Journal of Geophysical Research. Solid Earth, 122 (5): 3513-3539, Washington, DC: American Geophysical Union.

Adams, B.M., T.H. Kuehn, J.M. Bielicki, J.B. Randolph, and M.O. Saar (2014). On the importance of the thermosiphon effect in CPG (CO2 Plume Geothermal) power systems, Energy, DOI: 10.1016/j.energy.2014.03.032, 69:409-418.

Adams, B.M., T.H. Kuehn, J.M. Bielicki, J.B. Randolph, M.O. Saar (2015). A Comparison of Electric Power Output of CO_2 Plume Geothermal (CPG) and Brine Geothermal Systems for Varying Reservoir Conditions, Applied Energy, DOI: 10.1016/j.apenergy.2014.11.043, 140:365–377.

Ake J, Mahrer K, O'Connell D, Block L. (2005). Deep-Injection and Closely Monitored Induced Seismicity at Paradox Valley, Colorado. Bulletin of the Seismological Society of America, 95(2), 664–683. doi:10.1785/0120040072

Amitrano, D., and J. Schmittbuhl (2002), Fracture roughness and gouge distribution of a granite shear band, *J. Geophys. Res.*, *107*(B12), 2375 doi:10.1029/2002JB001761.

Amitrano, D., (2012). Variability in the power-law distributions of rupture events, Eur. Phys. J. Spec. Top., 205, 199–215.

Asanuma H, Soma N, Kaieda H, Kumano Y, Izumi T, Tezuka K, et al. (2005). Microseismic monitoring of hydraulic stimulation at the Australian HDR project in Cooper Basin. In Proceedings World Geothermal Congress (pp. 24–29).

Bachmann, C., S. Wiemer, J. Woessner, S. Hainzl (2011). Statistical analysis of the induced Basel 2006 earthquake sequence: Introducing a probability-based monitoring approach for Enhanced Geothermal Systems, Geophys. J. Int.

Bachmann, C., S. Wiemer, B. P. Goertz-Allmann, J. Woessner (2012). Influence of pore pressure on the size distribution of induced earthquakes, Geophysical Research Letters, 38, L09308.

Baisch, S., R. Weidler, R. Vörös, D. Wyborn, L. DeGraaf (2006). Induced seismicity during the stimulation of a geothermal HFR reservoir in the Cooper Basin (Australia), Bull. Seismol. Soc. Am. 96, no. 6, 2242–2256.

Baisch, S., R. Vörös, R. Weidler, D. Wyborn (2009). Investigation of fault mechanisms during geothermal reservoir stimulation experiments in the Cooper Basin (Australia), Bull. Seismol. Soc. Am. 99, no. 1, 148–158.

Baisch, S., Vörös, R., Rothert, E., Stang, H., Jung, R. Schellschmidt, R., (2010). A numerical model for fluid injection induced seismicity at Soutz-sous-Forêt, Int. J. Rock Mech. Min. Sci., 47, 405–413.Baisch, S., Harjes, H.P. (2003). A model for fluid-injection-induced seismicity at the KTB, Germany. Geophysical Journal International 152, 160–170.

Baisch, S., Rothert, E., Stang, H., Vörös, R., Koch, Ch., McMahon, A. (2015). Continued Geothermal Reservoir Stimulation Experiments in the Cooper Basin (Australia). Bulletin of the Seismological Society of America, Vol. 105, No. 1, pp. 198–209

Bandis S., A.C. Lumsden, N. R. Barton (1983). Fundamentals of rock joint deformation. International Journal of Rock Mechanics Mining Sciences & Geomech Abstr., 20, 6: 249–268.

Bao X., Eaton D. W. (2016). Fault activation by hydraulic fracturing in western Canada. Science 10.1126/science.aag2583

Baria, R., and A. S. P. Green (1986), Seismicity induced during a viscous stimulation at the Camborne School of Mines Hot Dry Rock Geothermal Energy project in Cornwall, England, paper presented at 8th Int. Acoustic Emission Symp., Japanese Soc. of NDI, Tokyo, Japan, October.

Barton, N.A., Choubey, V. (1977). The shear strength of rock joints in theory and practice. Rock Mechanics 10, 1-34.

Barton N., S. Bandis, K. Bakhtar (1985). Strength, deformation and conductivity coupling of rock joints. Int. J. Rock Mech. Min. Sic. & Geomech. Abstr. 22, 121-140.

Barton C.A., M. D. Zoback, D. Moos (1995). Fluid-flow along potentially active faults in crystalline rock. Geology, 23, 8: 683–686

Barton, C.A., S. Hickman, R. Morin, M.D. Zoback, R. Benoit (1998). Reservoir-scale fracture permeability in the Dixie Valley, Nevada, Geothermal Field, paper 47371 presented at SPE/ISRM Eurock '98, Soc. of Pet. Eng., Trondheim, Norway.

Batchelor, A. S., R. Baria, and K. Hearn (1983), Monitoring the effects of hydraulic stimulation by microseismic event location: a case study, in *58th Ann. Tech. Conf. and Exhibition of SPE*, edited, Soc. Petrol. Eng., San Francisco, California.

Baujard, C., Bruel, D., (2006). Numerical study of the impact of fluid density on the pressure distribution and stimulated volume in the Soultz HDR reservoir, Geothermics, 35, 607–621.

Bennour Z, Ishida T, Nagaya Y, Chen Y, Nara Y, Chen Q, Sekine K, Nagano Y (2015) Crack extension in hydraulic fracturing of shale cores using viscous oil, water, and liquid carbon dioxide. Rock Mech Rock Eng 48(4):1463–1473

Biot, M.A. (1941). General theory of three-dimensional consolidation. Journal of Applied Physics. 12: 155–164.

Blake, K., and N. Davatzes (2011), Crustal stress heterogeneity in the vicinity of COCO geothermal field, CA., paper presented at 36th Workshop on Geothermal Reservoir Engineering, Stanford University, Stanford University, Jan31-Feb2.

Block L., Wood C., Yeck W., King V. (2015). Induced seismicity constraints on subsurface geological structure, Paradox Valley, Colorado. Geophysical Journal International, 200(2), 1170–1193. doi:10.1093/gji/ggu459

Bommer, J.J., Oates, S., Cepeda, J.M., Lindholm, C., Bird, J., Torres, R., Marroqu´ın, G., Rivas, J., (2006). Control of hazard due to seismicity induced by a hot fractured rock geothermal project, Eng. Geol., 83, 287–306.

Boroumand N, Eaton D. (2012). Comparing Energy Calculations - Hydraulic Fracturing and Microseismic Monitoring. Presented at the Geoconvention 2012 - 74th Mtg., EAGE, Copenhagen, C042.

Breede, K., Dzebisashvili, K., Liu, X., and Falcone, G. (2013). A systematic review of enhanced (or engineered) geothermal systems: past, present and future. Geothermal Energy, 1(1):1.

Brown, D.W., (2000). A hot dry rock geothermal energy concept utilizing supercritical CO2 instead of water. In: Proceedings of the Twenty-Fifth Workshop on Geothermal Reservoir Engineering, Stanford, CA. Stanford University.

Brown, D. W., Duchane, D. V., Heiken, G., and Hriscu, V. T. (2012). Mining the Earth's heat: hot dry rock geothermal energy. Springer Science & Business Media.

Bruno M, Nakagawa F. (1991). Pore pressure influence on tensile fracture propagation in sedimentary rock. International Journal of Rock Mechanics and Mining Sciences & Geomechanics Abstracts, 28(4), 261–273. doi:10.1016/0148-9062(91)90593-b

Bunger A, Detournay E, Garagash D, Peirce A, others. (2007). Numerical simulation of hydraulic fracturing in the viscosity dominated regime. In SPE Hydraulic Fracturing Technology Conference. Society of Petroleum Engineers.

Bunger AP, Jeffrey RG, Kear J, Zhang X. (2011). Experimental Investigation of the Interaction among Closely Spaced Hydraulic Fractures. In 45th US Rock Mechanics / Geomechanics Symposium (pp. 11–318+). San Francisco.

Buscheck, T.A., J.M. Bielicki, T.A. Edmunds, Y. Hao, Y. Sun, J.B. Randolph, and M.O. Saar (2016). Multifluid geo-energy systems: Using geologic CO_2 storage for geothermal energy production and grid-scale energy storage in sedimentary basins, Geosphere, DOI: 10.1130/GES01207.1, 12(3):678-696.

Byerlee, J. (1978). Friction of rocks. Pure and applied geophysics, 116(4-5):615-626.

Caine, J. S., Evans, J. P., and Forster, C. B. (1996). Fault zone architecture and permeability structure. Geology, 24(11):1025-1028.

Calò, M., Dorbath, C., Cornet, F. H., & Cuenot, N. (2011). Large-scale aseismic motion identified through 4-DP-wave tomography. Geophysical Journal International, 186(3), 1295-1314.

Candela, T., Brodsky, E. E., Marone, C., & Elsworth, D. (2014). Laboratory evidence for particle mobilization as a mechanism for permeability enhancement via dynamic stressing. Earth and Planetary Science Letters, 392, 279-291.

Catalli, F., M.-A. Meier, S. Wiemer (2013). Coulomb stress changes at the Basel geothermal site: can the Coulomb model explain induced seismicity in an EGS? Geophys. Res. Let., 40.

Chacón E, Barrera V, Jeffrey R, van As A. (2004). Hydraulic fracturing used to precondition ore and reduce fragment size for block caving. Presented at the MassMin 2004 Santiago Chile.

Chen, Z., S. P. Narayan, Z. Yang, and S. S. Rahman (2000), An experimental investigation of hydraulic behaviour of fractures and joints in granitic rock, *Int. J. Rock Mech. & Min. Sci.*, *37*, 1061-1071.

Chitrala, Y., C. Moreno, C. H. Sondergeld, and C. S. Rai (2010), Microseismic mapping of laboratory induced hydraulic fractures in anisotropic reservoirs, paper presented at Tight Gas Completions Conference, Society of Petroleum Engineers.

Cornet, F. H., and J. Desroches (1989), The problem of channeling in Hot Dry Rock reservoirs, paper presented at Camborne School of Mines Intenational Hot Dry Rock Conference, Robertson Scientific Publishers, Llandudno, UK, Cornwall, UK.

Cornet, F. H., and O. Scotti (1993), Analysis of induced seismicity for fault zone identification, *Int. J. Rock Mech. Min. Sci. & Geomech. Abst.*, *30*(7), 789-795.

Cornet, F. H., and R. H. Jones (1994), Field evidence on the orientation of forced water flow with respect to the regional principal stress directions, paper presented at 1st North American Rock Mechanics Symposium, Balkema, Austin, Texas.

Cornet F. H., Helm J., Poitrenaud H., Etchecopar A. (1997). Seismic and Aseismic Slips Induced by Large-scale Fluid Injections. Pure appl. geophys. 150 (1997) 563–583

Cornet F.H., Li L., Hulin J.-P., Ippolito I., Kurowski P. (2003). The hydromechanical behaviour of a fracture: an in situ experimental case study. International Journal of Rock Mechanics & Mining Sciences 40 (2003) 1257–1270

Cornet, F.H. (2012). The relationship between seismic and aseismic motions induced by forced fluid injections. Hydrogeology Journal 20: 1463–1466.

Das I, Zoback MD. (2011). Long-period, long-duration seismic events during hydraulic fracture stimulation of a shale gas reservoir. The Leading Edge, 30(7), 778–786. doi:10.1190/1.3609093

Davies, R., Foulger, G., Bindley, A., Styles, P. (2013). Induced seismicity and hydraulic fracturing for the recovery of hydrocarbons, Marine and Petroleum Geology, 45, 171-185.

Deichmann, N., J. Ernst (2009). Earthquake focal mechanisms of the induced seismicity in 2006 and 2007 below Basel (Switzerland), Swiss J Geosci, 102(3), 457-466.

Deichmann, N., Kraft, T., Evans, K.F, (2014). Identification of faults activated during the stimulation of the Basel geothermal project from cluster analysis and focal mechanisms of the larger magnitude events. Geothermics, 52 (2014) 84–97.

Derode B., F. Cappa, Y. Guglielmi, J. Rutqvist (2013). Coupled seismo-hydromechanical monitoring of inelastic effects on injection-induced fracture permeability. International Journal of Rock Mechanics & Mining Sciences 61: 266–274

Detournay, E. (2016). Mechanics of Hydraulic Fractures. In Davis, SH and Moin, P, (eds), Annual Review of Fluid Mechanics, vol 48, p. 311-339.

Dusseault MB, McLennan J, Shu J. (2011). Massive multi-stage hydraulic fracturing for oil and gas recovery from low mobility reservoirs in China. Petroleum Drilling Techniques, 39(3), 6–16.

Edwards, B., Kraft, T., Cauzzi, C., Kaestli, P., and Wiemer, S. (2015). Seismic monitoring and analysis of deep geothermal projects in St Gallen and Basel, Switzerland. Geophysical Journal International, 201(2):1020-1037.

Ellsworth, W.L. (2013). Injection-induced earthquakes. Science, 12, 341, 6142

Elsworth, D., Fang, Y., Gan, Q., Im, K. J., Ishibashi, T., & Guglielmi, Y. (2016). Induced seismicity in the development of EGS—benefits and drawbacks. In Rock Dynamics: From Research to Engineering: Proceedings of the 2nd International Conference on Rock Dynamics and Applications (p. 13). CRC Press.

Emmermann R, Lauterjung J. (1997). The German Continental Deep Drilling Program KTB: Overview and major results. J. Geophys. Res., 102(B8), 18179–18201. doi:10.1029/96jb03945

Esaki T., H. Hojo, T. Kimura, N. Kameda, E. (1991). Shear-Flow Coupling Test on Rock joints. Proceedings – Seventh International Congress on Rock Mechanics, Vol 1: Rock Mechanics and Environmental Protection.

Esaki, T., Du, S., Mitani, Y., Ikusada, K., Jing, L., (1999). Development of a shear-flow test apparatus and determination of coupled properties for a single rock joint, Int. J. Rock Mech. Min. Sci., 36, 641–650.

Evans, K. F. (1983), Some examples and implications of observed elastic deformations associated with the growth of hydraulic fractures in the Earth, paper presented at Workshop on Hydraulic Fracturing Stress Measurements, National Academy Press, Monterey, California.

Evans, K., Holzhausen, G. (1983). On the development of shallow hydraulic fractures as viewed through the surface deformation field: Part 2-case histories. Journal of Petroleum Technology, 35(02):411-420.

Evans K.F., F. Wyatt (1984). Water table effects on the measurement of earth strain. Tectonophysics, 108: 323-337

Evans K.F., T. Kohl, L. Rybach, R.J. Hopkirk (1992). The effect of fracture normal compliance on the long-term circulation behaviour of a hot dry rock reservoir: A parameter study using the new fully coupled code fracture. Geothermal Resources Council Transactions, Vol. 16, 449-456, San Diego, CA

Evans, K. F., and P. Meier (1995), Hydro-jacking and hydrofracturing tests in a fissile schist in south-west Switzerland: In-situ stress characterisation in difficult rock, paper presented at 2nd Int. Conf. on the Mechanics of Jointed and Faulted Rock, Balkema, Vienna, 10-14 April.

Evans, J.P., Forster, C.B., Goddard, J.V. (1997). Permeability of fault-related rocks, and implications for hydraulic structure of fault zones. J. Struct. Geol. 19, 1393–1404.

Evans, K. F. (1998). Does significant aseismic slip occur on fractures in HDR systems under stimulation conditions? Proceedings, 4th Int. HDR Forum Strasbourg, September 28-30th. http://www.geothermal.ethz.ch/content/Geothermal%20publications/Evans_1998_4thHDRforum.pdf

Evans K. F., F. H. Cornet, T. Hashida, K. Hayashi, T. Ito, K. Matsuki, T. Wallroth (1999). Stress and rock mechanics issues of relevance to HDR/HWR engineered geothermal systems: review of developments during the past 15 years. Geothermics 28, 455-474

Evans K.F. (2005). Permeability creation and damage due to massive fluid injections into granite at 3.5 km at Soultz: 2. Critical stress and fracture strength, J. geophys. Res., 110.

Evans K. F., H. Moriya, H. Niitsuma, R.H. Jones, W.S. Phillips, A. Genter, J. Sausse, R. Jung, R. Baria (2005a). Microseismicity and permeability enhancement of hydrogeologic structures during massive fluid injections into granite at 3 km depth at the Soultz HDR site, Geophys. J. Int., 160, 388–412.

Evans K.F., A. Genter, J. Sausse (2005b). Permeability creation and damage due to massive fluid injections into granite at 3.5 km at Soultz: 1. Borehole observations. J. geophys. Res., 110, B04203.

Evans, K. F., Zappone, A., Kraft, T., Deichmann, N., and F. Moia (2012). A survey of the induced seismic responses to fluid injection in geothermal and CO2 reservoirs in Europe. Geothermics, 41: 30-54.

Evans, K. F., and S. Sikaneta (2013), Characterisation of natural fractures and stress in the Basel reservoir from wellbore observations (Module 1), in *GEOTHERM: Geothermal Reservoir Processes: Research towards the creation and sustainable use of Enhanced Geothermal Systems*, edited by K. F. Evans, pp. 9-18, Swiss Federal Office of Energy Publication No 290900, Bern.

Evans, K., Wieland, U., Wiemer, S., Giardini D. (2014). Deep Geothermal Energy R&D Roadmap for Switzerland, 2014. http://www.sccersoe.ch/export/sites/sccersoe/aboutus/.galleries/dwn_roadmaps/DGE_Roadmap_2014_Complete.pdf

Evans, K. F. (2014), Reservoir Creation, in Energy from the Earth - Deep Geothermal as a Resource for the Future?, edited by S. Hirschberg, S. Wiemer and P. Burgherr, pp. 82-118, Zentrum für Technologiefolgen-Abschätzung, Bern.

Eyre, T. S., and M. van der Baan (2015), Overview of moment-tensor inversion of microseismic events, *The Leading Edge*, *August*, 882-888 doi: 10.1190/tle34080882.1.

Fang, Y., Elsworth, D., Wang, C., Ishibashi, T., & Fitts, J. P. (2017). Frictional stability-permeability relationships for fractures in shales. Journal of Geophysical Research: Solid Earth, 122(3), 1760-1776.

Fang, Y., Elsworth, D., & Cladouhos, T. T. (2018). Reservoir permeability mapping using microearthquake data. Geothermics, 72, 83-100.

Faulkner D.R., and E.H. Rutter (2008). Can the maintenance of overpressured fluids in large strike-slip fault zones explain their apparent weakness? Geology 29, no. 6: 503–506.

Faulkner D., Jackson, C., Lunn, R., Schlische, R., Shipton, Z., Wibberley, C., Withjack, M., (2010). A review of recent developments concerning the structure, mechanics and fluid flow properties of fault zones. J. Struct. Geol. 32, 1557–1575.

Gale, J. E. (1975). A numerical, field and laboratory study of flow in rocks with deformable fractures. Ph.D. dissertation, Berkeley, University of California, 255 p.

Gale, J. E. (1993). Fracture properties from laboratory and large scale field tests: evidence of scale effects. Scale Effects in Rock Masses. Proc. 2nd Int. Workshop on Scale Effects in Rock Masses (Edited by Pinto da Cunha A.), Lisbon, pp. 341-352. Balkema, Rotterdam.

Garagash, D.I., L.N., Germanovich (2012). Nucleation and arrest of dynamic slip on a pressurized fault, J. Geophys. Res., 117, B10310.

Garapati, N., J.B. Randolph, and M.O. Saar (2015). Brine displacement by CO_2, energy extraction rates, and lifespan of a CO_2-limited CO_2 Plume Geothermal (CPG) system with a horizontal production well, Geothermics, DOI: 10.1016/j.geothermics.2015.02.005, 55:182–194.

Garcia, J., Walters, M., Beall, J., Hartline, C., Pingol, A., Pistone, S., & Wright, M. (2012, January). Overview of the northwest Geysers EGS demonstration project. In Proceedings, Thirty-Seventh Workshop on Geothermal Reservoir Engineering Stanford University.

Gentier, S., D. Hopkins, and J. Riss (2000). Role of fracture geometry in the evolution of flow paths under stress, in Dynamics of Fluids in Fractured Rock, Geophys. Monogr. Ser., vol. 122, edited by B. Faybishenko, P. A. Witherspoon, and S. M. Benson, pp. 169 – 184, AGU, Washington, D. C.

Genter A. , Goerke X., Graff J.-J, Cuenot N., Krall G., Schindler M., Ravier G. (2010). Current Status of the EGS Soultz Geothermal Project (France). Proceedings World Geothermal Congress 2010, Bali, Indonesia, 25-29 April 2010

Giardini, D. (2009). Geothermal quake risks must be faced, Nature, 462 (7275), 848-849.

Gischig, V.S., Wiemer, S. (2013). A stochastic model for induced seismicity based on non-linear pressure diffusion and irreversible permeability enhancement, Geophys. J. Int., 194(2), 1229–1249.

Gischig, V. S., Wiemer, S. Alcolea, A. R. (2014). Balancing reservoir creation and seismic hazard in enhanced geothermal systems. Geophysical Journal International. doi: 10.1093/gji/ggu221

Gischig, V. S. (2015). Rupture propagation behavior and the largest possible earthquake induced by fuid injection into deep reservoirs. Geophysical Research Letters, 42(18):7420-7428.

Gischig, V., G. Preisig (2015). Hydro-fracturing versus hydro-shearing: a critical assessment of two distinct reservoir stimulation mechanisms, paper presented at International Congress of Rock Mechanics, ISRM 2015, Montréal, Canada.

Gischig, V., Jalali, M., Amann, F., Krietsch, H., Klepikova, M., Esposito, S., Broccardo, M., Obermann, A., Mignan, A., Doetsch, J., Madonna, C. (2016). Impact of the ISC Experiment at the Grimsel Test Site-Assessment of Potential Seismic Hazard and Disturbances to Nearby Experiments and KWO Infrastructure. ETH Zurich, https://doi.org/10.3929/ethz-b-000189973.

Gischig, V.S., J. Doetsch, H. Maurer, H. Krietsch, F. Amann, K.F. Evans, M. Nejati, M.R. Jalali, A. Obermann, B. Valley, S. Wiemer, and D. Giardini (2017). On the link between stress field and small-scale hydraulic fracture growth in anisotropic rock derived from mirco-seismicity. Solid Earth.

Goebel, T. H. W., T. W. Becker, D. Schorlemmer, S. Stanchits, C. Sammis, E. Rybacki, G. Dresen (2012). Identifying fault heterogeneity through mapping spatial anomalies in acoustic emission statistics, J. Geophys. Res., 117, B03310.

Goertz-Allmann, B.P.,Goertz, A., Wiemer, S. (2011). Stress drop variations of induced earthquakes at the Basel geothermal site, Geophys. Res. Lett. 38(9), L09308.

Goertz-Allmann, B.P., Wiemer, S. (2013). Geomechanical modeling of induced seismicity source parameters and implications for seismic hazard assessment, Geophysics, 78(1), KS25–KS39.

Goodman R. E. (1974). The mechanical properties of joints. Proceedings of the 3rd Int. Congr. International Society of Rock Mechanics, Denver, Colorado. National Academy of Sciences, Washington, DC, I, 127–140.

Guglielmi, Y., F. Cappa, J. Rutqvist, C.-F. Tsang, and A. Thoraval (2006), Field and numerical investigations of free-water surface oscillation effects on rock slope hydromechanical behaviour – consequences for rock slope stability analyses paper presented at GEOPROC 2006: 2nd International Conference on Coupled Thermo-hydro-mechanicalchemical

Guglielmi Y., F. Cappa, J. Rutqvist, C.-F. Tsang, A. Thoraval (2008). Mesoscale characterization of coupled hydromechanical behavior of a fractured-porous slope in response to free water-surface movement. Int. J. Rock. Mech. Min. Sci. 42: 852–878.

Guglielmi Y., F. Cappa, H. Lancon, J. B. Janowczyk, J. Rutqvist, C. F. Tsang, J. S. Y. Wang (2014). ISRM Suggested Method for Step-Rate Injection Method for Fracture In-Situ Properties (SIMFIP): Using a 3-Components Borehole Deformation Sensor. Rock Mech. Rock Eng. 47: 303–311

Guglielmi, Y., Cappa, F., Avouac, J.-P., Henry, P., and Elsworth, D. (2015). Seismicity triggered by fuid injection induced aseismic slip. Science, 348(6240):1224-1226.

Guglielmi, Y.G. and Henry, P. Nussbaum, C. Dick, P. Gout, C. Amann, F. (2015). Underground Research Laboratories for conducting fault activation experiments in shales. 49th US Rock Mechanics / Geomechanics Symposium held in San Francisco, CA, USA, ARMA 15-0489

Gupta, H. K. (1992), *Reservoir-induced Earthquakes*, 364 pp., Elsevier, Amsterdam, The Netherlands.

Haimson, B. C., and F. H. Cornet (2003), ISRM suggested methods for rock stress estimation-Part 3: hydraulic fracture (HF) and/or hydraulic testing of pre-existing fractures (HTPF), *Int. J. Rock Mech. Min. Sci.*, *40*, 1011-1020.

Hampton, J. C., L. Matzar, D. Hu, and M. Gutierrez (2015), Fracture dimension investigation of laboratory hydraulic fracture interaction with natural discontinuity using acoustic emission, paper presented at 49th US Rock Mechanics/Geomechanics Symposium, Americal Rock Mechanics Association, San Francisco, 28 June-1 July.

Häring, M.O., Schanz, U., Ladner, F. & Dyer, B.C., (2008). Characterization of the Basel 1 enhanced geothermal system, Geothermics, 37, 469–495.

Healy, J. H., W. W. Rubey, D. T. Griggs, and C. B. Raleigh (1968), The Denver earthquakes, *Science*, *161*, 1301-1310.

Hickman, S., M. D. Zoback, and R. Benoit (1998), Tectonic controls on fault-zone permeability in a geothermal reservoir at Dixie Valley, Nevada, paper 47213 presented at SPE/ISRM Eurock '98, Soc. of Pet. Eng., Trondheim, Norway.

Hickman, S. H., M. Zoback, C. A. Barton, R. Benoit, J. Svitek, Summer, and R. (2000), Stress and permeability heterogeneity within the Dixie Valley geothermal reservoir: recent results from well 82-5, paper presented at Twenty-Fifth Workshop on Geothermal Reservoir Engineering, Stanford University, Stanford University, Stanford, CA, Jan 24-26.

Hogarth, R., H. Holl, and A. McMahon (2013), Flow testing results from Habanero EGS Project, paper presented at Australian Geothermal Energy Conferences, Brisbane, Australia, 14-15 November.

Horálek, J., Z. Jechumtálová, L. Dorbath, and J. Síleny (2010), Source mechanisms of micro-earthquakes induced in a fluid injection experiment at the HDR site Soultz-sous-Forˆets (Alsace) in 2003 and their temporal and spatial variations, *Geophys. J. Int.*, *181*, 1547-1565 doi: 10.1111/j.1365-246X.2010.04506.x.

Houben, G. (2015), Review: Hydraulics of water wells—flow laws and influence of geometry, *Hydrogeology J.*, *23*, 1633-1657.

Hubbert, M. K. and Rubey, W. W. (1959). Role of uid pressure in mechanics of overthrust faulting i. mechanics of uid-_lled porous solids and its application to overthrust faulting. Geological Society of America Bulletin, 70(2):115{166.

Hummel, N., and T. M. Müller (2009), Microseismic signatures of non-linear pore-fluid pressure diffusion, Geophys. J. Int., 179, 1558-1565 doi: 10.1111/j.1365-246X.2009.04373.x.

Husen, S., C. Bachmann, D. Giardini (2007). Locally triggered seismicity in the central Swiss Alps following the large rainfall event of August 2005. Geophysical Journal International, 171 (2007), pp. 1126-1134, 10.1111/j.1365-246X.2007.03561.x

Huw, C., Eisner, L., Styles, P., Turner, P., (2014). Felt seismicity associated with shale gas hydraulic fracturing: The first documented example in Europe, Geophysical Research Letter, doi: 10.1002/2014GL062047

Ishida T. (2001). Acoustic emission monitoring of hydraulic fracturing in laboratory and field. Construction and Building Materials 15 Ž2001. 283-295

Jaeger JC. (1963). Extension Failures in Rocks subject to fluid Pressure. Journal of Geophysical Research, 68(21), 6066–6067.

Jeanne, P., Y. Guglielmi, and F. Cappa. 2012. Dissimilar properties within a carbonate-reservoir's small fault zone, and their impact on the pressurization and leakage associated with CO2 injection. Journal of Structural Geology. DOI:10.1016/j.jsg.2012.10.010

Jeanne, P., Rutqvist, J., Vasco, D., Garcia, J., Dobson, P. F., Walters, M., Hartline, C., Borgia, A. (2014). A 3D hydrogeological and geomechanical model of an Enhanced Geothermal System at The Geysers, California. Geothermics, 51, 240-252.

Jeanne, P., Rutqvist, J., Rinaldi, A. P., Dobson, P. F., Walters, M., Hartline, C., & Garcia, J. (2015). Seismic and aseismic deformations and impact on reservoir permeability: The case of EGS stimulation at The Geysers, California, USA. Journal of Geophysical Research: Solid Earth, 120(11), 7863-7882.

Jeffrey RG, Brynes RP, Lynch PJ, Ling DJ. (1992). An Analysis of Hydraulic Fracture and Mineback Data for a Treatment in the German Creek Coal Seam. Society of Petroleum Engineers. doi:10.2118/24362-MS

Jeffrey R, Enever J, Phillips R, Ferguson T, Davidson S, Bride J. (1993). Small-Scale Hydraulic Fracturing and Mineback Experiment in Coal Seams. Presented at the Proceedings of the 1993 International Coalbed methane Symposium.

Jeffrey RG, Settari A. (1995). A Comparison of Hydraulic Fracture Field Experiments, Including Mineback Geometry Data, with Numerical Fracture Model Simulations. Society of Petroleum Engineers. doi:10.2118/30508-MS

Jeffrey RG, Bunger A. (2007). A Detailed Comparison of Experimental and Numerical Data on Hydraulic Fracture Height Growth Through Stress Contrasts. Society of Petroleum Engineers. doi:10.2118/106030-MS

Jeffrey RG, Bunger AP, Lecampion B, Zhang X, Chen ZR, van As A, et al. (2009). Measuring Hydraulic Fracture Growth in Naturally Fractured Rock. In 2009 SPE Annual Technical Conference and Exhibition (p. SPE 124919+). New Orleans, Louisiana, USA: SPE.

Johnson E, Cleary MP. (1991). Implications of recent laboratory experimental results for hydraulic fractures. Society of Petroleum Engineers. doi:10.2118/21846-MS

Jost M, Büßelberg T, Jost Ö, Harjes H. (1998). Source parameters of injection-induced microearthquakes at 9 km depth at the KTB Deep Drilling site, Germany. Bulletin of the Seismological Society of America, 88(3), 815–832.

Jung R. (1989). Hydraulic in situ investigations of an artificial fracture in the Falkenberg Granite. Int. J. Rock Mech. Min. Sci. & Geomech. Abstr. 26: 301-308.

Jung R. (2013). EGS — Goodbye or Back to the Future. Effective and Sustainable Hydraulic Fracturing, http://dx.doi.org/10.5772/56458

Jupe A. Green A. S. P., Wallroth T. (1992). Induced Microseismicity and Reservoir Growth at the Fjällbacka Hot Dry Rocks Project, Sweden. Int. J. Rock Mech. Min. Sci. & Geomech. Abstr. Vol. 29. No. 4. pp. 343-354.

Kaieda, H., Jones, R., Moriya, H., Sasaki, S. & Ushijima, K., (2005). Ogachi HDR reservoir evaluation by AE and geophysical methods, in Proceedings of World Geothermal Congress 2005, Antalya, Turkey, April 24–29.

Karvounis, D.C., Gischig, V.S., Wiemer, S., (2014). Towards a Real-Time Forecast of Induced Seismicity for Enhanced Geothermal Systems. Proceedings of the 2014 Shale Energy Engineering Conference, July 21–23, 2014, Pittsburgh, Pennsylvania, 246.

Keranen, K., M, Savage, H. M., Abers, G. A., & Cochran, E. S. (2013). Potentially induced earthquakes in Oklahoma, USA: Links between wastewater injection and the 2011 Mw 5.7 earthquake sequence, Geology 41 (6), 699–702, doi:10.1130/G34045.1

Keusen, H.R., Ganguin, J., Schuler, P., Buletti, M., 1989. Grimsel test site: Geology. Nationale Genossenschaft fuer die Lagerung Radioaktiver Abfaelle (NAGRA), Baden, Switzerland. Technical Report NTB 87-14E, 166 pp.

Király, E., Zechar, J.D., Gischig, V.S, Karvounis, D., Doetsch, J., Wiemer, S., (2015). Modeling Induced Seismicity and Validating Models in Deep Geothermal Energy Projects. In preparation.

Kohl, T., K. F. Evans, R. J. Hopkirk, R. Jung, and L. Rybach (1997), Observation and simulation of non-Darcian flow transients in fractured rock, *Wat. Resourc. Res.*, *33*(3), 407-418.

Krietsch, H., V. Gischig, R. Jalali, F. Amann, K. F. Evans, J. Doetsch, and B. Valley (2017), Stress measurements in crystalline rock: Comparison of overcoring, hydraulic fracturing and induced seismicity results, in *ARMA 51st US Rock Mechanics / Geomechanics Symposium*, edited, San Francisco, California, USA.

Lee, H. S., and T. F. Cho (2002), Hydraulic Characteristics of Rough Fractures in Linear Flow under Normal and Shear Load, *Rock Mech. Rock Eng.*, *35*, 299-318 DOI 10.1007/s00603-002-0028-y.

Lee, H.S., Cho, T.F. (2002). Hydraulic characteristics of rough fractures in linear flow under normal and shear load, Rock Mech. Rock Eng., 35(4), 299–318.

Louis, C., J.-L., Dessene, B. Feuga (1977). Interaction between water flow phenomena and the mechanical behavior of soil or rock masses. Gudehns, G., ed., Finite elements in geomechanics: New York, John Wiley S Sons, 572 p.

Majer, E., J. Nelson, A. Robertson-Tait, J. Savy, and I. Wong (2012). Protocol for addressing induced seismicity associated with enhanced geothermal systems, U.S. Department of Energy, Energy Efficiency and Renewable Energy.

Manning, C. and Ingebritsen, S. (1999). Permeability of the continental crust: Implications of geothermal data and metamorphic systems. Reviews of Geophysics, 37(1):127/150.

Marone, C., and C. H. Scholz (1988), The depth of seismic faulting and the upper transition from stable to unstable slip regimes, *Geophys. Res. Lett.*, *15*(6), 621-624 DOI: 10.1029/GL015i006p00621.

Martínez-Garzón, P., Bohnhoff, M., Kwiatek, G., & Dresen, G. (2013). Stress tensor changes related to fluid injection at The Geysers geothermal field, California. Geophysical Research Letters, 40(11), 2596-2601.

Martínez-Garzón, P., Kwiatek, G., Bohnhoff, M., & Dresen, G. (2017). Volumetric components in the earthquake source related to fluid injection and stress state. Geophysical Research Letters, 44(2), 800-809.

Martin C. D., C. C. Davison, E. T. Kozak (1990). Characterizing normal stiffness and hydraulic conductivity of a major shear zone in granite. Rock joints, eds. Barton & Stephansson, Balkema, Rotterdam, Netherlands.

Maury, V., 1994. Rock failure mechanisms identification: A key for wellbore stability and reservoir behaviour problem, in Eurock 94, edited by Delft, Netherlands, 29-31 August, 175-182, Balkema.

Maxwell, S. (2014), Microseismic Imaging of Hydraulic Fracturing: Improved Engineering of Unconventional Shale Reservoirs, 197 pp., Society of Exploration Geophysicists.

McClure M.W., R. N. Horne (2011). Investigation of injection-induced seismicity using a coupled fluid flow and rate/state friction model. Geophysics 76, 6.

McClure M.W., R. N. Horne (2014). An investigation of stimulation mechanisms in Enhanced Geothermal Systems International Journal of Rock Mechanics & Mining Sciences 72: 242–260

McClure, M. W. (2012). Modeling and characterization of hydraulic stimulation and induced seismicity in geothermal and shale gas reservoirs. PhD thesis, Stanford University.

McClure, M. W. (2015), Generation of large postinjection-induced seismic events by backflow from dead-end faults and fractures, Geophysical Research Letters, 42(6647–6654).

McGarr, A. (1976). Seismic moments and volume changes, Journal of Geophysical Research, 81(8), 1487-1494.

Mena, B.,Wiemer, S., Bachmann, C., (2013). Building robust model to forecast the induced seismicity related to geothermal reservoir enhancements, Bull. seism. Soc. Am., 103(1), 383–393.

Meng, C. (2011), Hydraulic fracture propagation in pre-fractured rocks, paper presented at SPE Hydraulic Fracturing Technology Conference and Exhebition, SPE, The Woodlands, Texas, 24-26 Jan.

Mignan, A., Landtwing, D., Kästli, P., Mena, B., Wiemer, S. (2015). Induced seismicity risk analysis of the 2006 Basel, Switzerland, Enhanced Geothermal System project: Influence of uncertainties on risk mitigation, Geothermics, 53 (2015) 133–146.

Murdoch LC, Schweisinger T, Svenson E, Germanovich L. (2004). Measuring and analyzing transient changes in fracture aperture during well tests: preliminary results. In: Dynamics of fluids in fractured rock (Witherspoon Conference). LBL Report 54275, February 10–14, 2004. p. 129–32.

Murphy H., C. Huang, Z. Dash, G. Zyvoloski, A. White (2004). Semi-analytical solutions for fluid flow in rock joints with pressure-dependent openings. Water Resources Research 40, W12506

Nicholson, C., and R. L. Wesson (1990), Earthquake Hazard Associated with Deep Well Injection-A Report to the U.S. Environmental Protection Agency, 1951, US Geological Survey Bulletin.

Nicol, D. A. C., and B. A. Robinson (1990), Modelling the heat extraction from the Rosemanowes HDR reservoir, *Geothermics*, *19*, 247-257.

Niitsuma H., M. Fehler, R. Jones, S. Wilson, J. Albright, A. Green, R. Baria, K. Hayashi, H. Kaieda, K. Tezuka, A. Jupe, T. Wallroth, F. Cornet, H. Asanuma, H. Moriya, K. Nagano, W.S. Phillips, J. Rutledge, L. House, A. Beauce, D. Alde, R. Aster (1999). Current status of seismic and borehole measurements for HDR/HWR development. Geothermics, 28, 4-5: 475-490.

Olsson R., N. Barton (2001). An improved model for hydromechanical coupling during shearing of rock joints. International Journal of Rock Mechanics and Mining Sciences, 38, 3: 317–329.

Parker R. (1999). The Rosemanowes HDR project 1983-1991. Geothermics, 28, 603-615.

Parker, R. H. (1989a), Hot Dry Rock Geothermal Energy: Phase 2B Final Report of the Camborne School of Mines Project, 1391 pp., Pergamon Press, Oxford.

Pearson, C. (1981), The relationship between microseismicity and high pore pressures during hydraulic stimulation experiments in low porosity granitic rock, *J. Geophys. Res.*, *86*, 7855-7864.

Pettitt W, Pierce M, Damjanac B, Hazzard J, Lorig L, Fairhurst C, et al. (2011). Fracture network engineering for hydraulic fracturing. The Leading Edge, 30(8), 844–853. doi:10.1190/1.3626490

Petty, S., Nordin, Y., Glassely, W., Cladouhos, T. (2013). Improving geothermal project economics with multi-zone stimulation: results from the Newberry volcano EGS demonstration. Proc. 38th Works. Geoth. Rese. Eng., Stanford University, SGP-TR-198.

Phillips, S., L. S. House, and M. C. Fehler (1997), Detailed joint structure in a geothermal reservoir from studies of induced microseismic clusters, *J. Geophys. Res.*, *102*(B6), 11,745-711,763.

Pine, R.J., Baria, R., Pearson, R.A., Kwakwa, K., McCartney, R (1987). A Technical Summary of Phase 2B of the Camborne School of Mines HDR Project, 1983-1986. Geothermics, 16, 4: 341-353.

Potter, R., Robinson, E., and Smith, M. (1974). Method of extracting heat from dry geothermal reservoirs. US Patent 3,786,858.

Power, W. L., and T. E. Tullis (1991), Euclidean and fractal models for the description of surface roughness, *J. Geophys. Res.*, *96*(B1), 415-424.

Preisig, G., E. Eberhardt, V. Gischig, V. Roche, M. Van der Baan, B. Valley, P. Kaiser, and D. Du (2015), Development of connected rock mass permeability by hydraulic fractures growth accompanying fluid injection, Geofluids 15, 321–337. Rahman, M.K., Hossain, M.M., Rahman, S.S. (2002). A shear-dilation-based model for evaluation of hydraulically stimulated naturally fractured reservoirs. International Journal for Numerical and Analytical Methods in Geomechanics, 26, 5: 469-497.

Pruess, K., (2006). Enhanced geothermal systems (EGS) using CO2 as working fluid – a novel approach for generating renewable energy with simultaneous sequestration of carbon. Geothermics 35 (4), 351–367.

Pruess, K., (2007). Role of fluid pressure in the production behavior of enhanced geothermal systems with CO2 as working fluid. GRC Trans. 31, 307–311.

Raleigh, C., Healy, J., and Bredehoeft, J. (1976). An experiment in earthquake control at rangely, colorado. work (Fig. Ib), 108(52):30.

Randolph, J.B., and M.O. Saar (2011a), Combining geothermal energy capture with geologic carbon dioxide sequestration, Geophysical Research Letters, DOI: 10.1029/2011GL047265, 38, L10401.

Randolph, J.B. and M.O. Saar (2011b). Coupling carbon dioxide sequestration with geothermal energy capture in naturally permeable, porous geologic formations: Implications for CO_2 sequestration, Energy Procedia, DOI: 10.1016/j.egypro.2011.02.108, 4:2206-2213.

Rutledge, J. T., Phillips, W. S., & Mayerhofer, M. J.: Faulting Induced by Forced Fluid Injection and Fluid Flow Forced by Faulting: An Interpretation of Hydraulic-Fracture Microseismicity, Carthage Cotton Valley Gas Field, Texas, Bulletin of the Seismological Society of America, 94, (2004),1817.

Rutqvist J. (1995): Determination of hydraulic normal stiffness of fractures in hard rock from well testing. Int. J. Rock Mech. Min. Sci.1, 32: 513–23.

Rutqvist, J., and O. Stephansson (1996), A cyclic hydraulic jacking test to determine the in-situ stress normal to a fracture, *Int. J. Rock Mech. Min. Sci. & Geomech. Abstr.*, *33*(7), 695-711.

Rutqvist J., O. Stephansson (2003). The role of hydromechanical coupling in fractured rock engineering. Hydrogeology Journal, 11, 1:7–40.

Rutqvist, J., and C. M. Oldenburg (2008), Analysis of injection-induced micro-earthquakes in a geothermal stream reservoir, Geysers Geothermal Field, California, Proceedings of the 42th U. S. Rock Mechanics Symposium, June 29–July 2, 2008, San Francisco, California, USA, 151.

Rutqvist, J. (2011). Status of the tough-ac simulator and recent applications related to coupled fluid flow and crustal deformations. Computers & Geosciences, 37(6):739-750.

Saar, M.O., and M. Manga (2003). Seismicity induced by seasonal groundwater recharge at Mt. Hood, Oregon, Earth and Planetary Science Letters, DOI: 10.1016/S0012-821X(03)00418-7, 214:605-618.

Saar, M.O., and M. Manga (2004). Depth dependence of permeability in the Oregon Cascades inferred from hydrogeologic, thermal, seismic, and magmatic modeling constraints, Journal of Geophysical Research, DOI: 10.1029/2003JB002855, 109, Nr. B4, B04204.

Saar, M.O. (2011). Review: Geothermal heat as a tracer of large-scale groundwater flow and as a means to determine permeability fields, Hydrogeology Journal, DOI: 10.1007/s10040-010-0657-2, 19:31-52, 2011.

Saar, M.O. (2017). Novel Geothermal Technologies, in Potentials, costs and environmental assessment of electricity generation technologies, edited by C. Bauer and S. Hirschberg, Swiss Federal Office of Energy, Swiss Competences Center for Energy Research "Supply of Electricity", Swiss Competence Center for Energy Research "Biomass for Swiss Energy Future".

Samuelson, J., Elsworth, D., & Marone, C. (2009). Shear-induced dilatancy of fluid□saturated faults: Experiment and theory. Journal of Geophysical Research: Solid Earth, 114(B12).

Schanz U, Dyer B, Ladner F, Haering MO. (2007). Microseismic aspects of the Basel 1 geothermal reservoir. In 5th Swiss Geoscience Meeting. Geneva.

Schmittbuhl, J., F. Schmitt, and C. H. Scholz (1995), Scaling invariance of crack surfaces, *J. Geophys. Res.*, *100*(B4), 5953-5973.

Schoenball, M., Baujard, C., Kohl, T., Dorbath, L. (2012). The role of triggering by static stress transfer during geothermal reservoir stimulation, J. geophys. Res., 117, B09307.

Scholz, C. H. (2015), On the stress dependence of the earthquake b value, *Geophys. Res.Lett.*, *42*, 1399-1402 doi:10.1002/2014GL062863.

Scholz, C.H., 1990. The mechanics of Earthquakes and Faulting. Cambridge University Press, Cambridge, UK, p. 39.

Schorlemmer, D., S. Wiemer, Wyss, M., (2005). Variations in earthquake size distribution across different stress regimes, Nature, 437, 539–542.

Schrauf T. W., Evans D. D. (1986). Laboratory Studies of Gas Flow Through a Single Natural Fracture WATER RESOURCES RESEARCH, VOL. 22, NO. 7, 1038-1050

Schweisinger T., E.J. Swenson, L.C. Murdoch (2009): Introduction to hydromechanical well tests in fractured rock aquifers. Groundwater 47, 1:69–79

Schweisinger, T., L.C. Murdoch, and C.O. Huey Jr. (2007). Design of a removable borehole extensometer. Geotechnical Testing Journal 30, no. 3: 202–211.

Scotti O., Cornet F.H. (1994). In situ evidence for fluid induced aseismic slip events along fault zones. Int J Rock Mech Min 1:347-358.

Shamir, G., and M. D. Zoback (1992), Stress orientation profile to 3.5 km depth near the San Andreas fault at Cajon Pass, California, *J. Geophys. Res.*, *97*, 5059-5080.

Sileny, J., D. P. Hill, and F. H. Cornet (2009), Non–double-couple mechanisms of microearthquakes induced by hydraulic fracturing, *J. Geophys. Res.*, *114*, B08307 doi:10.1029/2008JB005987.

Song I, Suh M, Won K, Haimson B. (2001). A laboratory study of hydraulic fracturing breakdown pressure in tablerock sandstone. Geosciences Journal, 5(3), 263–271. doi:10.1007/bf02910309

Spada, M., Tormann, T.,Goebel, T., Wiemer, S. (2013). Generic dependence of the frequency-size distribution of earthquakes on depth and its relation to the strength profile of the crust, Geophys. Res. Lett., 40(4), 709–714.

Stein, R. S. (1999). The role of stress transfer in earthquake occurrence. Nature, 402(6762): 605-609.

Tenma N., Yamaguchi T., Zyvoloski G. (2008). The Hijiori Hot Dry Rock test site, Japan evaluation and optimization of heat extraction from a two-layered reservoir. Geothermics 2008; 37:19–52.

Terakawa, T., Miller, S.A., Deichmann, N. (2012). High fluid pressure and triggered earthquakes in the enhanced geothermal system in Basel, Switzerland, J. Geophys. Res., 117, B07305.

Tester, J. W., Anderson, B. J., Batchelor, A., Blackwell, D., DiPippo, R., Drake, E., Garnish,J., Livesay, B., Moore, M., Nichols, K., et al. (2006). The future of geothermal energy. Impact of

Enhanced Geothermal Systems (EGS) on the United States in the 21st Century, Massachusetts Institute of Technology, Cambridge, MA, page 372.

Tezuka, K., and H. Niitsuma (2000), Stress estimated using microseismic clusters and its relationship to the fracture system of the Hijiori Hot Dry Rock reservoir, *Engineering Geology*, *56*, 47-62.

Tormann, T., B Enescu, J. Woessner and S. Wiemer (2015). Randomness of megathrust earthquakes implied by rapid stress recovery after the Japan earthquake, Nature Geoscience 8 (2), 152-158.

Tormann, T., S. Wiemer, A. Mignan (2014). Systematic survey of high-resolution b value imaging along Californian faults: Inference on asperities, J. Geophys. Res. Solid Earth, 119(3), 2029–2054.

Valley, B., and K. F. Evans (2009), Stress orientation to 5 km depth in the basement below Basel (Switzerland) from borehole failure analysis, *Swiss J. Earth Sci.*, *102*, 467-480 doi: 10.1007/s00015-009-1335-z.

Valley, B., and K. F. Evans (2010), Stress Heterogeneity in the Granite of the Soultz EGS Reservoir Inferred from Analysis of Wellbore Failure, paper presented at World Geothermal Congress, International Geothermal Association, Bali, 25-29 April 2010

van As A, Jeffrey RG. (2000). Caving Induced by Hydraulic Fracturing at Northparkes Mines. Presented at the 4th North American Rock Mechanics Symposium, American Rock Mechanics Association. https://www.onepetro.org/conference-paper/ARMA-2000-0353.

van As A, Jeffrey R. (2002). Hydraulic fracture growth in naturally fractured rock: mine through mapping and analyses. Presented at the NARMS-TAC conference, Toronto, Canada.

van As, A., Jeffrey R., Chacónn E. and Barrera, V. (2004). Preconditioning by hydraulic fracturing for bloc caving in a moderately stressed naturally fractured orebody. Proceeding of the Massmin 2004 conference, Santiago Chile, 22-25 August 2004.

van der Baan M, Eaton D, Dusseault M. (2013). Microseismic Monitoring Developments in Hydraulic Fracture Stimulation. In R Jeffrey (Ed.), Effective and Sustainable Hydraulic Fracturing. InTech. http://www.intechopen.com/books/effective-and-sustainable-hydraulic-fracturing/microseismic-monitoring-developments-in-hydraulic-fracture-stimulation.

Vermylen J, Zoback MD. (2011). Hydraulic Fracturing, Microseismic Magnitudes, and Stress Evolution in the Barnett Shale, Texas, USA. Society of Petroleum Engineers. doi:10.2118/140507-MS

Vogler D., Amann F., Bayer P., Elsworth D. (2015). Permeability Evolution in Natural Fractures Subject to Cyclic Loading and Gouge Formation. RMRE, 49(9).

Warpinski N. (2009). Microseismic Monitoring: Inside and Out. Journal of Petroleum Technology, 61(11), 80–85. doi:10.2118/118537-JPT

Warpinski NR, Clark JA, Schmidt RA, Huddle CW. (1982). Laboratory Investigation on the - Effect of In-Situ Stresses on Hydraulic Fracture Containment. Society of Petroleum Engineers Journal, 22(03), 333–340. doi:10.2118/9834-PA

Warpinski N., L. W. Teufel (1987): Influence of geologic discontinuities on hydraulic fracture propagation. J. Petrol. Technol. 39: 209–20

Warpinski NR, Du J. (2010). Source-Mechanism Studies on Microseismicity Induced by Hydraulic Fracturing. Society of Petroleum Engineers. doi:10.2118/135254-MS

Warpinski NR. (1985). Measurement of Width and Pressure in a Propagating Hydraulic Fracture. Society of Petroleum Engineers Journal, 25(01), 46–54. doi:10.2118/11648-PA

Warpinski N. (2013). Understanding Hydraulic Fracture Growth, Effectiveness, and Safety Through Microseismic Monitoring. In R Jeffrey (Ed.), Effective and Sustainable Hydraulic Fracturing. InTech. http://www.intechopen.com/books/effective-and-sustainable-hydraulic-fracturing/understanding-hydraulic-fracture-growth-effectiveness-and-safety-through-microseismic-monitoring.

Warren W. E., Schmith C. W. (1985). In Situ Stress Estimates From Hydraulic Fracturing and Direct Observation of Crack Orientation. Journal of Geophysical Research, Vol. 9, NO. B8, 829-68

Wehrens, P. (2015). Structural evolution in the Aar Massif (Haslital transect): Implications for the mid-crustal deformation. PhD thesis, University Bern.

Wolhart, S. L., T. A. Harting, J. E. Dahlem, T. Young, M. J. Mayerhofer, and E. P. Lolon (2006), Hydraulic fracture diagnostics used to optimize development in the Jonah field, paper presented at SPE Annual Technical Conference and Exhibition. Society of Petroleum Engineers.

Yeo I. W., M. H. De Freitas, and R. W. Zimmerman (1998). Effect of shear displacement on the aperture and permeability of a rock fracture. International Journal of Rock Mechanics and Mining Sciences, 35, 8:1051–1070

Yoon, J.-S., Zang, A., Stephansson, O., 2014. Numerical investigation on optimized stimulation of intact and naturally fractured deep geothermal reservoirs using hydro-mechanical coupled discrete particles joints model. Geothermics, 52.

Zang A, Yoon J.S., Stephansson O, Heidbach O. (2013). Fatigue hydraulic fracturing by cyclic reservoir treatment enhances permeability and reduces induced seismicity. Geophysical Journal International, 195(2), 1282–1287. doi:10.1093/gji/ggt301

Zang A., Stephansson O. (2013). Stress Field of the Earth's Crust. Springer Dordrecht Heidelberg London New York, DOI 10.1007/978-1-4020-8444-7.

Ziegler M, Valley B, Evans K. (2015). Characterisation of Natural Fractures and Fracture Zones of the Basel EGS Reservoir Inferred from Geophysical Logging of the Basel-1 Well. Presented at the Proceedings World Geothermal Congress 2015.

Zoback, M.D., Rummel, F., Jung R., Raleigh C.B. (1977). Laboratory Hydraulic Fracturing Experiments in Intact and Pre-fractured Rock Int. J. Rock Mech. Min. Sci. & Geomech. Abstr. Vol. 14, pp. 49-58.

Zoback, M. D. and Harjes, H.-P. (1997). Injection-induced earthquakes and crustal stress at 9 km depth at the KTB deep drilling site, Germany. Journal of Geophysical Research: Solid Earth, 102(B8):18477-18491.

Zoback, M. D., Kohli, A., Das, I., McClure, M. W., et al. (2012). The importance of slow slip on faults during hydraulic fracturing stimulation of shale gas reservoirs. In SPE Americas Unconventional Resources Conference. Society of Petroleum Engineers.

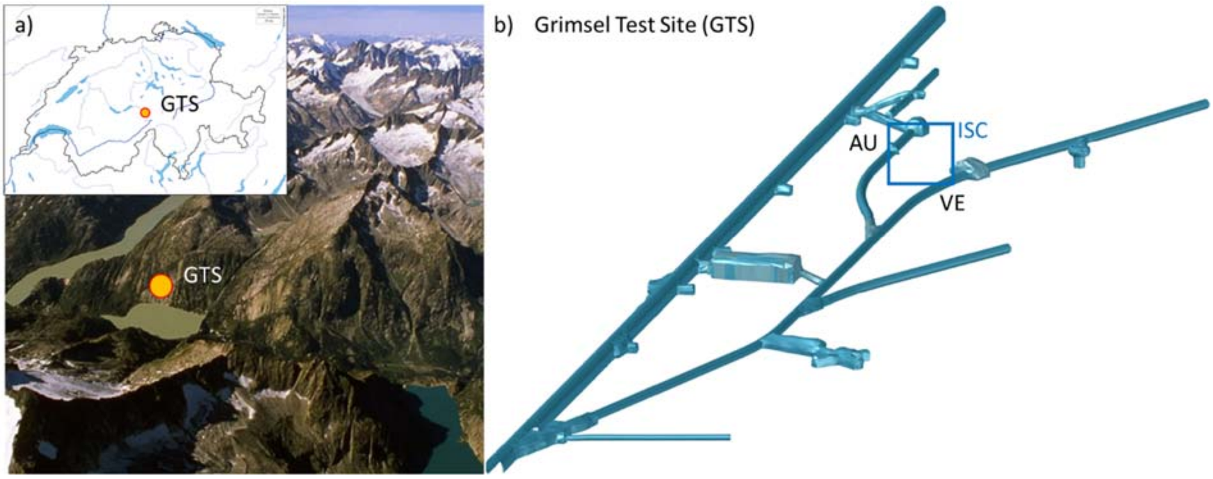

Figure 1. a) Grimsel Test Site (GTS) is located in the Swiss Alps in the central part of Switzerland. b) The in-situ stimulation and circulation experiment (ISC experiment) is implemented in the southern part of the GTS in a low fracture density granitic rock

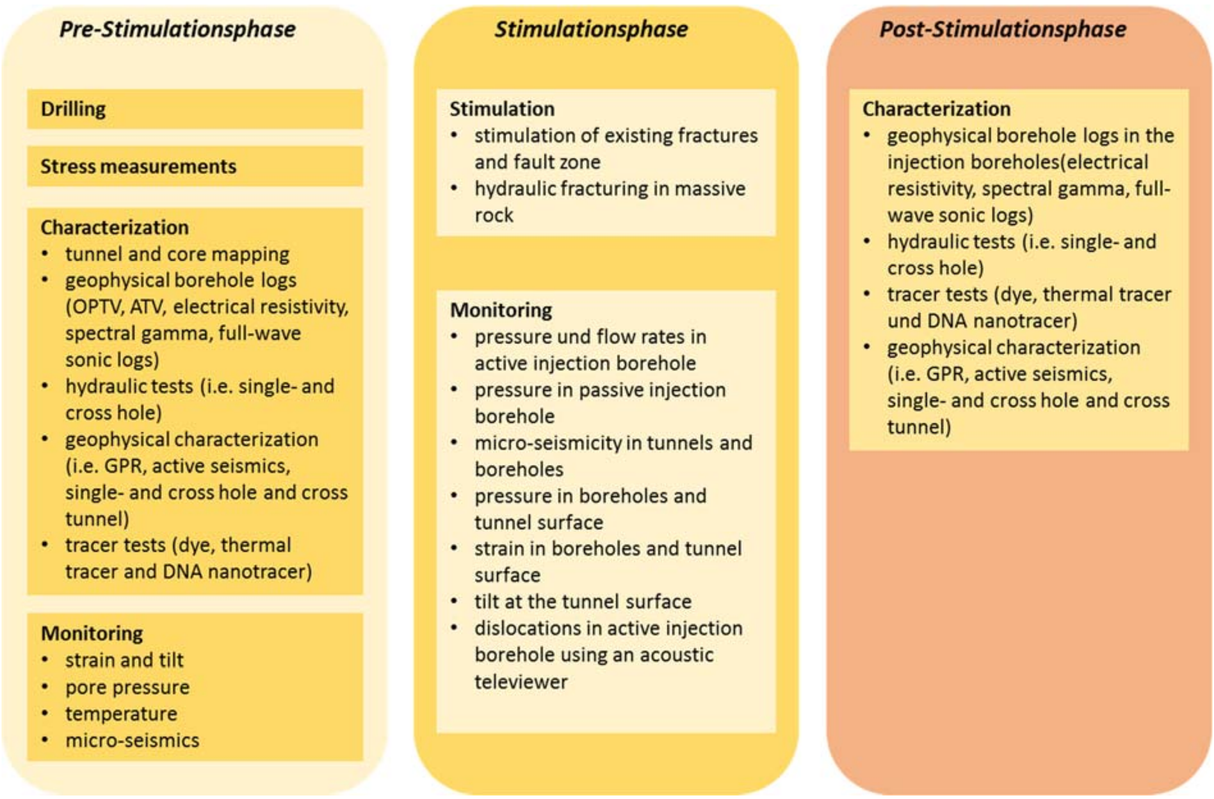

Figure 2. The three test phases of the ISC experiments with listings of the main activities during each phase.

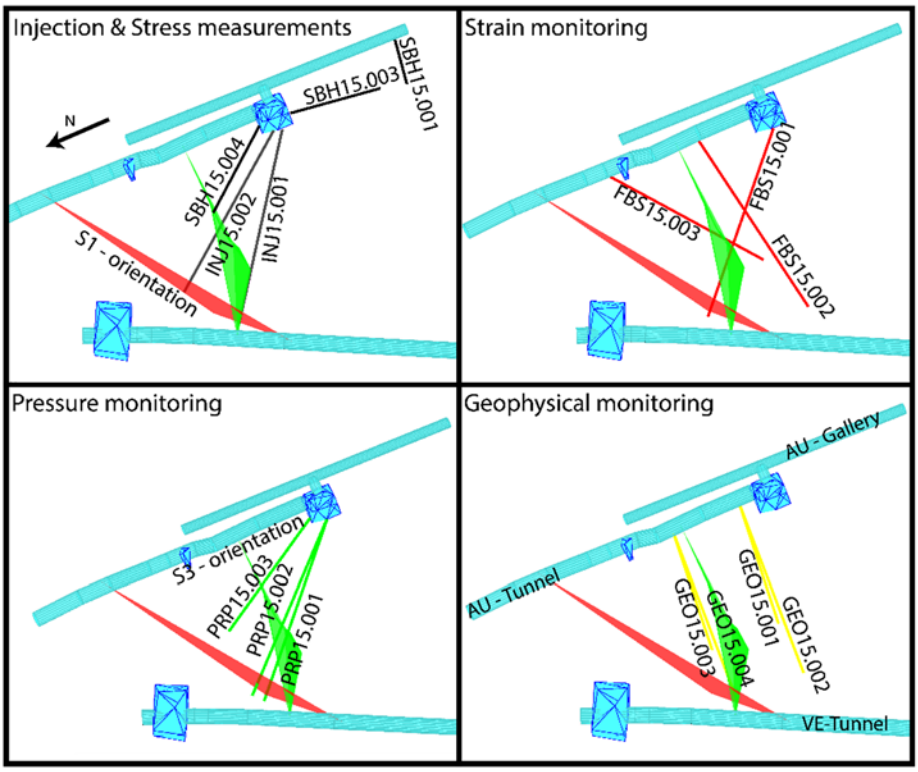

Figure 3: The 15 boreholes drilled for the ISC experiment (view steeply inclined towards SE).

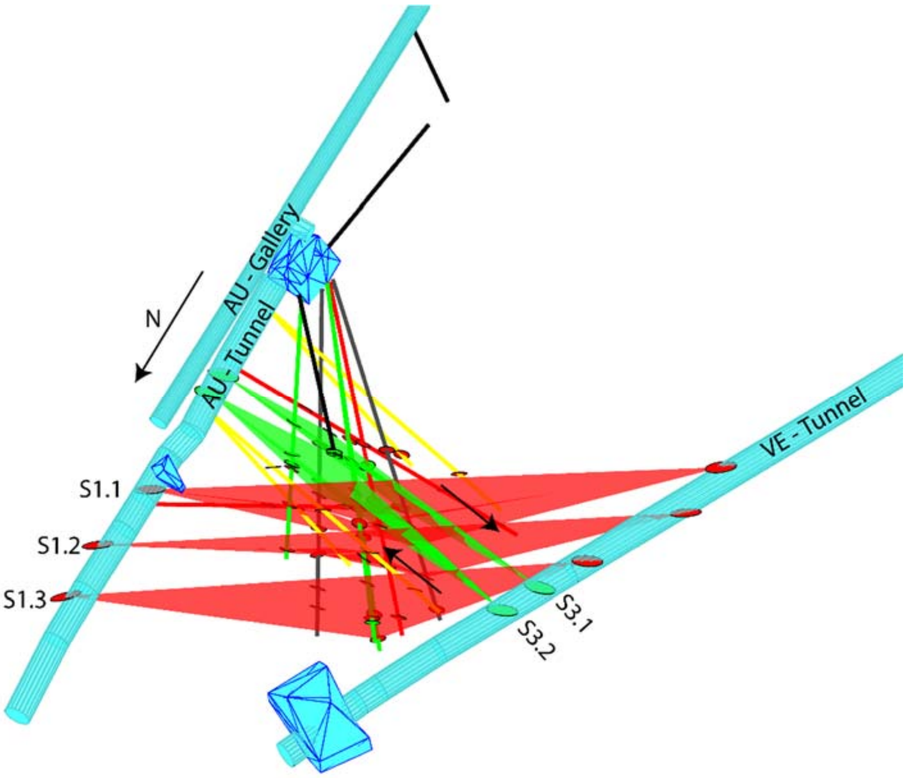

Figure 4: 3D-Model showing the boreholes drilled towards the rock volume for the in-situ stimulation experiment, S1 (red) and S3 (green) oriented shear zones as well as the dextral shear sense at the S3 shear zones indicated by the black arrows.

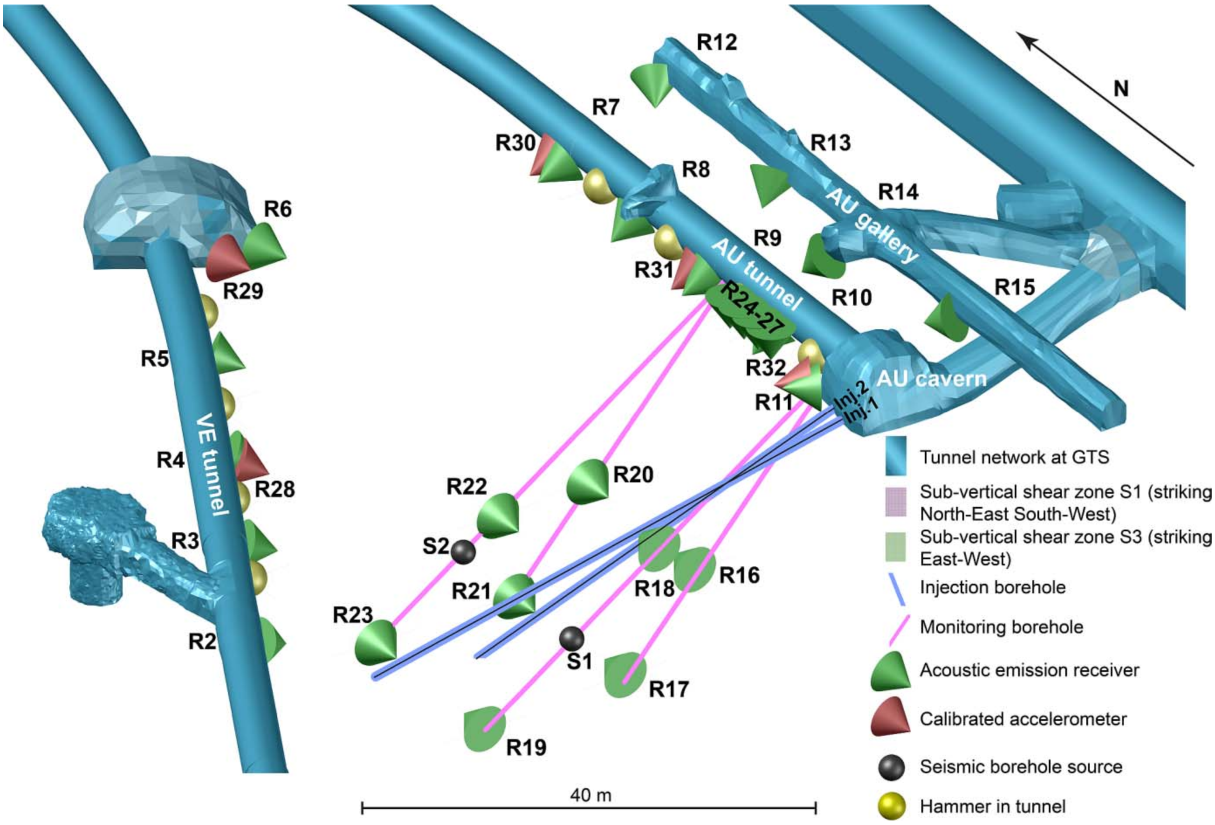

Figure 5: Outline of seismic monitoring network including hammer sources and borehole piezosources for active seismic surveys.

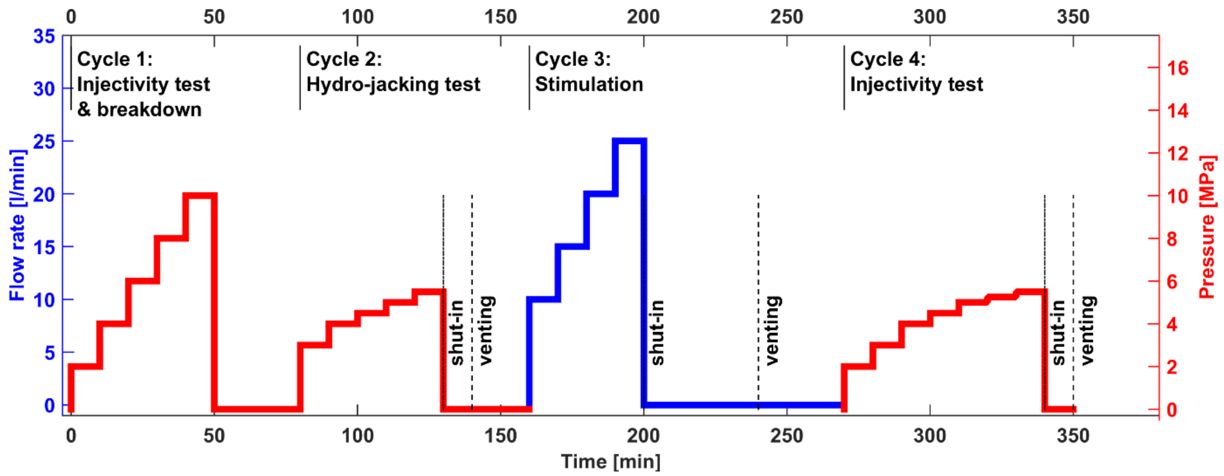

Figure 6: Injection protocol for hydroshearing experiments. Red curves denote pressure controlled injections (Cycle 1, 2 and 4), blue curves flow rate controlled injections (Cycle 3). The total volume injected is 1 m^3.

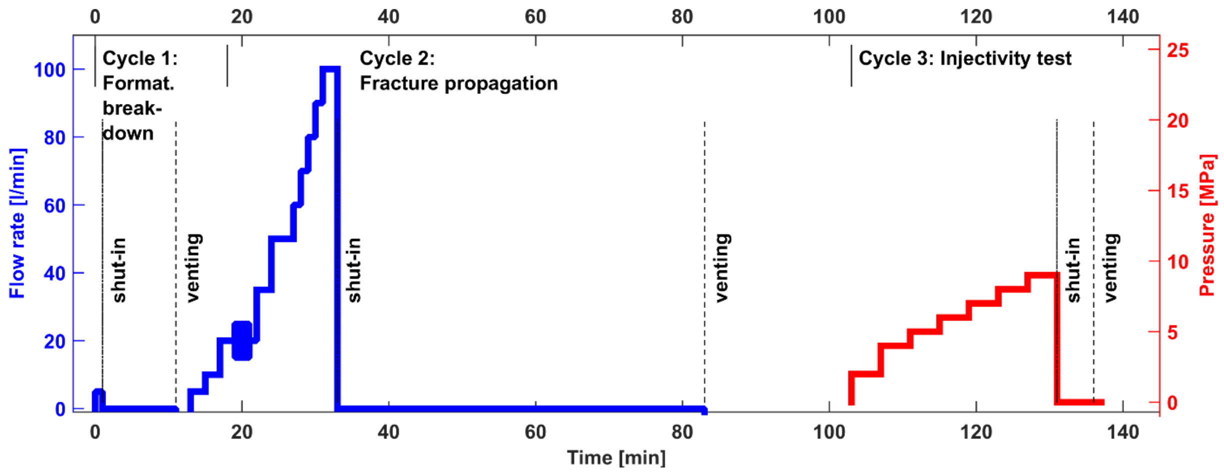

Figure 7: Injection protocol for hydrofracturing experiments. The blue solid curve denotes flow rate controlled and the red solid curve pressure controlled injection.